Quantum diffusion of massive Dirac fermions induced by symmetry breaking

Ting Zhang [1,2] Chushun Tian [3,*] and Ping Sheng [1,2]
[1] Department of Physics, Hong Kong University of Science and Technology, Clear Water Bay, Kowloon, Hong Kong, China
[2] Institute for Advanced Study, Hong Kong University of Science and Technology, Clear Water Bay, Kowloon, Hong Kong, China
[3] CAS Key Laboratory of Theoretical Physics and Institute of Theoretical Physics, Chinese Academy of Sciences, Beijing 100190, China

(Received 25 May 2020; revised 2 July 2021; accepted 26 July 2021; published 16 August 2021)

We show that when a two-dimensional (2D) Dirac fermion moves in disordered environments, the weak time-reversal symmetry breaking by a small mass gives rise to the diffusive wave propagation, i.e., that the wave-packet spread obeys the diffusive law of Einstein, up to a—practically inaccessible—exponentially large length. Strikingly, the diffusion constant is larger than that given by the Boltzmann kinetic theory, and grows unboundedly as the energy-to-mass ratio increases. This diffusive phenomenon is of quantum nature and different from weak antilocalization. It implies a new type of transport in topological insulators at zero temperature.

DOI: 10.1103/PhysRevB.104.075427

I. INTRODUCTION

A common wisdom brought by the discovery of localization in quantum disordered [1,2] and quantum chaotic [3,4] systems is that the diffusive law established by Einstein in 1905, i.e., the mean squared displacement grows linearly in time:

$$\langle \boldsymbol{r}^2 \rangle_t \sim Dt, \tag{1}$$

with D the diffusion constant, is not favored in the low-dimensional quantum world. The loss of the memory of particle's momentum due to collisions with scatterers can be remedied by various quantum ingredients, such as interference of quantum waves [5–7], quantum chaoticity of dynamics [8,9], and the exchange interaction between particles [10]. The memory recovery corrupts the foundation of Boltzmann kinetic theory for diffusion [11,12]. As a result, the linear scaling (1) is violated and the (normal) diffusion is suppressed. Should the temperature be finite, the quantum phase coherence is destroyed by thermal noises and diffusion can thus appear [13].

However, recent progresses achieved in very different research areas, ranging from quantum transport of superconducting films [14,15] to wave-packet dynamics of 2D quantum chaotic systems [16–18], have posed a fundamental challenge for the common wisdom. In particular, by using the field theory and the mathematical spectral theory, it is established that, when some canonical quantum chaotic systems are endowed with spin, the diffusive law (1) can persist in the entire course of wave-packet propagation at the critical point of topological phase transitions [16–18]. It is thus suggested that the arising of the irreversible diffusion can go far beyond the canonical Einstein-Boltzmann paradigm and may have novel quantum origin in the presence of spin.

In reality an important spin system is the 2D massive Dirac fermion, described by a two-component spinor $\psi(\boldsymbol{r}, t)$, which propagates according to the $(2+1)$D Dirac equation. It models a number of electronic materials including anomalous Hall systems [19], graphene in the spin-$\uparrow$ K valley gapped by a spin-orbit interaction [20]; and magnetically doped surface states of topological insulators [21–23]. These Dirac fermions carry rich spin properties [24]. It is natural to expect that when they move in a disordered environment, strong interplay between their spin properties and multiple random wave scattering may give rise to rich wave propagation phenomena. In particular, whether the diffusive law (1) emerges—at zero temperature—is of fundamental interest, and may find practical applications. It has been a long-term interest to generalize the Boltzmann equation to investigate the interplay between diffusion and various wave effects [25,26]. Recent nonperturbative studies [11,12,16–18] have suggested that to address the emergence of quantum diffusion it is crucial to go beyond traditional ladder and maximally crossing diagrams [2,5–8,21]. This turns out to be a highly nontrivial task, as general disordered Dirac systems are concerned. To the best of our knowledge, such task has been undertaken only for the limiting massless case [27]. But in that case, instead of Eq. (1), a superdiffusive propagation $\langle \boldsymbol{r}^2 \rangle_t \sim t \ln t$ was found, leading to topological metallic behaviors [28,29].

The above implies that the behaviors of massless Dirac materials and electronic materials with spin-orbit interaction [30,31] in disordered environments are completely different in the scaling characteristic of their conductance. This is the case even though both systems are in the same sympletic symmetry class and the same dimension (2D). The difference is especially striking in that for the former system the scaling law is found to be one-loop type even in the nonperturbative regime [27–29], and thus no localization transition occurs; this is in sharp contrast to the presence of localization transition in the latter system [31]. A problem arising thereby is what happens to massive Dirac particles, which no longer belongs to the sympletic symmetry class; this is the problem addressed in the present paper.

*ct@itp.ac.cn

II. SUMMARY OF MAIN RESULTS AND PHYSICAL PICTURE

In this paper we formulate a density response theory for 2D Dirac fermions of mass m moving in a disordered scalar potential, which allows us to address the propagation of wave packet. We focus on the case where the particle energy ε satisfies $\varepsilon/m \gg 1$ and $\varepsilon\tau \gg 1$, with τ the elastic scattering time, which is order of the Boltzmann collision time. (Both the velocity parameter and the Planck constant $\hbar$ are set to unity.) The two inequalities quantify the conditions of small mass and weak disorder, respectively. We find that, at zero temperature, quantum diffusion occurs at the time scale $\tau_m \equiv (\frac{\varepsilon}{m})^2\frac{\tau}{2}$, much larger than the time scale τ when the Boltzmann kinetic theory applies. Specifically, fluctuations in the particle number density relax according to the diffusion equation, that gives rise to the scaling law (1); however, the diffusion constant D is determined by a highly nonlinear equation:

$$\frac{D_0}{D} = 1 - \frac{1}{2\pi^2\nu}\int_0^{\frac{1}{\tau}} dQQ\frac{1}{\tau_m^{-1} + DQ^2}, \tag{2}$$

where the second term on the right hand side is of quantum origin, with ν the local density of state. It exceeds the Boltzmann diffusion constant $D_0 = \tau$, and grows unboundedly with the ratio $\frac{\varepsilon}{m}$. In two limiting regimes: (I) $\frac{\varepsilon}{m} \ll e^{\pi\varepsilon\tau}$ and (II) $\frac{\varepsilon}{m} \gg e^{\pi\varepsilon\tau}$, the explicit analytical expression of D reads:

$$D = \begin{cases} D_0 + \frac{1}{2\pi^2\nu}\ln\frac{\varepsilon}{\sqrt{2}m}, & \text{for regime I ;} \\ \frac{1}{2\pi^2\nu}\ln\frac{\varepsilon}{\sqrt{2}m}, & \text{for regime II.} \end{cases} \tag{3}$$

In the regime I, the quantum term $\frac{1}{2\pi^2\nu}\ln\frac{\varepsilon}{\sqrt{2}m}$ is $\ll D_0$ implying weak quantum diffusion; in the regime II, it is $\gg D_0$ implying strong quantum diffusion. The quantum term is completely determined by ν and ε/m, independent of the disorder parameter τ. Interestingly, it is reproduced when one replaces the logarithm $\ln\frac{L}{\tau}$ (with L being a length scale) in the conductivity for $m = 0$ [27–29] by $\ln\sqrt{\frac{\tau_m}{\tau}}$ (and uses the Einstein relation between the conductivity and the diffusion constant). Note that the one-loop weak antilocalization correction [30,32,33] corresponds only to the first line of Eq. (3), but not to the second. The latter is for the regime where the "correction" is $\gg D_0$, i.e., beyond the expected validity of the one-loop calculation as shown in Fig. 1, where quantum diffusion is shown to exist at $D \gg D_0$. We further show that the length scale to develop unitary class localization is exponentially large in $(\nu D)^2$, and thus all localization effects are invisible in practice. In contrast, the results shown in this paper are in the relevant length scales that are experimentally accessible.

Now we explain in a pictorial way that a small but nonvanishing m is the key to the emergence of quantum diffusion. First of all, when the particle moves in a disordered environment, random scattering by impurities renders the memory of momentum lost at the time scale τ, like in the canonical Einstein-Boltzmann paradigm. However, at longer times the memory gets recovered by constructive interference between different propagating paths of quantum waves. In combination with the helicity, that introduces strong spin-momentum locking, the memory recovery enhances the relaxation time of momentum and renormalizes τ: The more the memory is recovered, the slower the momentum relaxes. Then, as we will implement by a systematic analytical theory below, it turns out that on one hand the quantum interference rests on system's invariance under some time-reversal operation $\hat{T}$, while on the other hand this $\hat{T}$ symmetry is weakly broken by small m. As a result, the constructive interference and the ensuing memory recovery can persist only up to some time scale, which is τ_m. After that the particle undergoes random scattering again. So at the time scale of τ_m the wave-packet propagation is diffusive, but with the diffusion constant enhanced from D_0 by the memory recovery (Fig. 1).

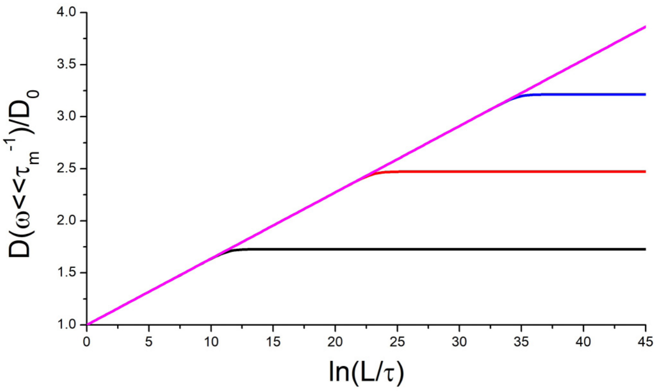

FIG. 1. Solving Eq. (19) numerically shows that as the length scale increases, the low-frequency diffusion constant increases from the Boltzmann value D_0 and levels off at a larger value—the quantum diffusion constant D obeying Eq. (2). Here $\varepsilon\tau = 5$ and from the bottom to the top $\varepsilon/m = 10^5, 10^{10}, 10^{15}, +\infty$.

III. OUTLINE OF ANALYTICAL THEORY

Now we outline the analytical derivations. The complete theory is given in the supplemental material [34] written in a self-contained and article style. The quantum wave propagates according to $\partial_t\psi = \hat{H}\psi$, $\hat{H} \equiv \boldsymbol{\sigma}\cdot\boldsymbol{p} + m\sigma^z + V(\boldsymbol{r})$ with $\boldsymbol{\sigma} \equiv (\sigma^x, \sigma^y)$, where $\sigma^{x,y,z}$ are the Pauli matrices and $\boldsymbol{p} \equiv -i\nabla$, $\boldsymbol{r}$ are the momentum and the position operator, respectively. The disordered potential $V(\boldsymbol{r})$ has a zero mean everywhere, and its fluctuations are spatially independent, i.e., $\langle V(\boldsymbol{r})V(\boldsymbol{r}')\rangle = U_0\delta(\boldsymbol{r}-\boldsymbol{r}')$ with $\langle\cdot\rangle$ denoting the average over disorder configurations. Here U_0 is the disorder strength and can be expressed as $U_0 = 1/(\pi\nu\tau)$. Note that U_0, ε, m are renormalized at short scales [19]. But the renormalized values enter into the large-scale physics discussed below merely as parameters. So we will not discuss this further.

Introducing the time-reversal operation $\hat{T} := -i\sigma^y\hat{C}$, where $\hat{C}$ stands for the complex conjugation and applying it to $\hat{H}$, we find that

$$\begin{aligned} &for\, m = 0:\ \hat{T}\hat{H}\hat{T}^{-1} = \hat{H}; \\ &for\, m \neq 0:\ \hat{T}\hat{H}\hat{T}^{-1} \neq \hat{H}. \end{aligned} \tag{4}$$

That is, for $m = 0$ the system has the time-reversal symmetry, otherwise the symmetry is broken. For $m \ll \varepsilon$, in which we are interested, the breaking is weak, and the field theory developed for strong $\hat{T}$-symmetry breaking (i.e., the unitary class) [35] does not apply.

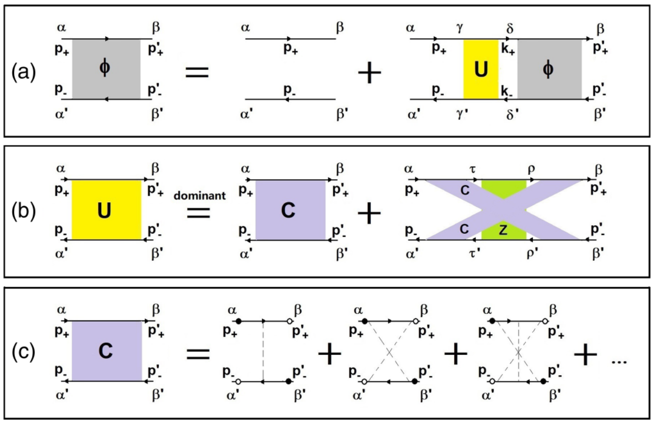

FIG. 2. The diagrammatical representation of the Bethe-Salpeter equation for the response function ϕ (a); the dominant contributions to the two-particle irreducible vertex function U (b); and the singlet cooperon C (c). In (b) the diagrammatical structure of Z is arbitrary. In (c) the solid (respectively empty) circles stand for that two end spins are paired into a singlet state.

The program to be executed below is in spirit parallel to the theory for localization of spinless particles [6,7]. However, some key steps are renovated by generalizing the treatments developed for massless Dirac fermions [27] to the massive case. Most importantly, the final results have totally opposite physical implications. Define the retarded (advanced) 2×2 matrix Green function as $G_\varepsilon^{R(A)} := 1/(\varepsilon - \hat{H} \pm i\delta)$, with δ a positive infinitesimal. Then the motion of Dirac fermions over large length and time scales can be characterized by the response function,

$$\sum_{\boldsymbol{p},\boldsymbol{p}',\boldsymbol{q}} e^{i(\boldsymbol{p}_+\cdot\boldsymbol{r}_+ - \boldsymbol{p}'_+\cdot\boldsymbol{r}'_+ + \boldsymbol{p}'_-\cdot\boldsymbol{r}'_- - \boldsymbol{p}_-\cdot\boldsymbol{r}_-)}\phi^{\boldsymbol{p}\boldsymbol{p}'}_{\alpha\beta,\beta'\alpha'}(\boldsymbol{q},\omega)$$
$$:= -\frac{1}{2\pi i}\big\langle (G^R_{\varepsilon_+}(\boldsymbol{r}_+,\boldsymbol{r}'_+))_{\alpha\beta}(G^A_{\varepsilon_-}(\boldsymbol{r}'_-,\boldsymbol{r}_-))_{\beta'\alpha'}\big\rangle. \qquad (5)$$

Here $\boldsymbol{p}_\pm = \boldsymbol{p} \pm \frac{\boldsymbol{q}}{2}$, $\boldsymbol{p}'_\pm = \boldsymbol{p}' \pm \frac{\boldsymbol{q}}{2}$, $\varepsilon_\pm = \varepsilon \pm \frac{\omega}{2}$, and $\alpha, \beta, \ldots$ are spin indices to which the Einstein summation convention applies below. Upon performing the disorder averaging, the translational invariance is restored, and the right-hand side depends only on three independent coordinates: $\frac{\boldsymbol{r}_+ + \boldsymbol{r}_-}{2} - \frac{\boldsymbol{r}'_+ + \boldsymbol{r}'_-}{2}$, $\boldsymbol{r}_+ - \boldsymbol{r}_-$, $\boldsymbol{r}'_- - \boldsymbol{r}'_+$. The Fourier wavenumbers, $\boldsymbol{q}, \boldsymbol{p}, \boldsymbol{p}'$, respectively, conjugate to them.

When we expand $G_\varepsilon^{R,A}$ in V and perform the disorder averaging, each term of $\phi^{\boldsymbol{p}\boldsymbol{p}'}_{\alpha\beta,\beta'\alpha'}$ is mapped onto a specific diagram. As shown in Fig. 2(a), the backbone of each diagram consists of two particle lines: the upper (lower) particle line corresponds to $G^{R(A)}$. The building blocks of each diagram are the free Green functions $\mathcal{G}_\varepsilon^{R(A)}(\boldsymbol{r}-\boldsymbol{r}') := \langle G_\varepsilon^{R(A)}(\boldsymbol{r},\boldsymbol{r}')\rangle$, represented by a solid line going rightwards (leftwards), and the disorder scattering $U_0\delta(\boldsymbol{r}-\boldsymbol{r}')$, represented by a dashed line. In the Fourier representation, $\mathcal{G}_\varepsilon^{R(A)}$ has the general form: $\mathcal{G}_\varepsilon^{R(A)}(\boldsymbol{p}) = (\varepsilon - \boldsymbol{\sigma}\cdot\boldsymbol{p} - m\sigma^z - \Sigma_\varepsilon^{R(A)}(\boldsymbol{p}))^{-1}$, where $\Sigma_\varepsilon^{R(A)}$ is the self-energy. All diagrams of the response function can be organized in the way shown by Fig. 2(a), which is described by the Bethe-Salpeter equation:

$$\phi^{\boldsymbol{p}\boldsymbol{p}'}_{\alpha\beta,\beta'\alpha'}(\boldsymbol{q},\omega) = (\mathcal{G}^R_{\varepsilon_+}(\boldsymbol{p}_+))_{\alpha\gamma}(\mathcal{G}^A_{\varepsilon_-}(\boldsymbol{p}_-))_{\gamma'\alpha'}\Bigg(-\frac{\delta_{\boldsymbol{p}\boldsymbol{p}'}\delta_{\gamma\beta}\delta_{\beta'\gamma'}}{2\pi i}$$
$$+\sum_{\boldsymbol{k}} U^{\boldsymbol{p}\boldsymbol{k}}_{\gamma\delta,\delta'\gamma'}(\boldsymbol{q},\omega)\phi^{\boldsymbol{k}\boldsymbol{p}'}_{\delta\beta,\beta'\delta'}(\boldsymbol{q},\omega)\Bigg). \qquad (6)$$

Here the kernel U is a two-particle irreducible vertex function. As exemplified by Fig. 2(c), each diagram of U has ends joined by the disorder scattering line, and cannot be divided into disconnected parts through cutting the upper and the lower particle line simultaneously. Furthermore, by adapting the method of Ref. [36] it can be shown that U obeys the Ward identity:

$$\sum_{\boldsymbol{p}} (\delta\mathcal{G}_\varepsilon(\boldsymbol{p}))_{\gamma'\gamma} U^{\boldsymbol{p}\boldsymbol{k}}_{\gamma\delta,\delta'\gamma'} = (\delta\Sigma_\varepsilon(\boldsymbol{k}))_{\delta'\delta}, \qquad (7)$$

where $\delta\mathcal{G}_\varepsilon(\boldsymbol{p}) := \mathcal{G}^R_{\varepsilon_+}(\boldsymbol{p}_+) - \mathcal{G}^A_\varepsilon(\boldsymbol{p}_-)$ and $\delta\Sigma_\varepsilon(\boldsymbol{p})$ is defined in the similar way. Equations (6) and (7) are rigorous, laying down a foundation for the analysis of the density response of massive Dirac fermions.

Multiplying both sides of Eq. (6) by the inverse of the matrix $\mathcal{G}^R$, we obtain

$$\big(\varepsilon_+ - \boldsymbol{\sigma}\cdot\boldsymbol{p}_+ - m\sigma^z - \Sigma^R_{\varepsilon_+}(\boldsymbol{p}_+)\big)_{\gamma\alpha}\phi^{\boldsymbol{p}\boldsymbol{p}'}_{\alpha\beta,\beta'\alpha'}$$
$$= \big(\mathcal{G}^A_{\varepsilon_-}(\boldsymbol{p}_-)\big)_{\gamma'\alpha'}\Bigg(-\frac{\delta_{\boldsymbol{p}\boldsymbol{p}'}\delta_{\gamma\beta}\delta_{\beta'\gamma'}}{2\pi i} + \sum_{\boldsymbol{k}} U^{\boldsymbol{p}\boldsymbol{k}}_{\gamma\delta,\delta'\gamma'}\phi^{\boldsymbol{k}\boldsymbol{p}'}_{\delta\beta,\beta'\delta'}\Bigg), \qquad (8)$$

and similarly, we have

$$\big(\varepsilon_- - \boldsymbol{\sigma}\cdot\boldsymbol{p}_- - m\sigma^z - \Sigma^A_{\varepsilon_-}(\boldsymbol{p}_-)\big)_{\alpha'\gamma'}\phi^{\boldsymbol{p}\boldsymbol{p}'}_{\alpha\beta,\beta'\alpha'}$$
$$= \big(\mathcal{G}^R_{\varepsilon_+}(\boldsymbol{p}_+)\big)_{\alpha\gamma}\Bigg(-\frac{\delta_{\boldsymbol{p}\boldsymbol{p}'}\delta_{\gamma\beta}\delta_{\beta'\gamma'}}{2\pi i} + \sum_{\boldsymbol{k}} U^{\boldsymbol{p}\boldsymbol{k}}_{\gamma\delta,\delta'\gamma'}\phi^{\boldsymbol{k}\boldsymbol{p}'}_{\delta\beta,\beta'\delta'}\Bigg), \qquad (9)$$

where the arguments $\boldsymbol{q}, \omega$ are suppressed in order to make the formulas compact. Let us set $\beta = \beta'$ in both equations, set $\gamma = \alpha'$ in the first equation and $\gamma' = \alpha$ in the second, and sum up the spin indices and the momenta. Subtracting the two equations thereby obtained and using Eq. (7), we obtain the macroscopic equation describing the particle number conservation:

$$-i\omega\phi_0(\boldsymbol{q},\omega) + i\boldsymbol{q}\cdot\boldsymbol{\phi}_j(\boldsymbol{q},\omega) = i\nu. \qquad (10)$$

Here $i\nu$ is the source. ϕ_0 and $\boldsymbol{\phi}_j$ are the density and the current relaxation function, respectively, whose microscopic expressions are

$$\phi_0 = \sum_{\boldsymbol{p},\boldsymbol{p}'}\phi^{\boldsymbol{p}\boldsymbol{p}'}_{\alpha\beta,\beta\alpha}, \quad \boldsymbol{\phi}_j = \sum_{\boldsymbol{p},\boldsymbol{p}'}\boldsymbol{\sigma}_{\alpha'\alpha}\phi^{\boldsymbol{p}\boldsymbol{p}'}_{\alpha\beta,\beta\alpha'}. \qquad (11)$$

It should be emphasized that Eqs. (10) and (11) are exact, irrespective of the disorder strength, i.e., $\varepsilon\tau$. That they follow from Eqs. (8) and (9) is in spirit similar to that hydrodynamic equations follow from the Boltzmann kinetic equation. Should an additional relation between ϕ_0 and $\boldsymbol{\phi}_j$ exist, then the macroscopic equation (10) is closed.

Now we establish such a relation for $\varepsilon\tau \gg 1$. Note that the diagrams dominating $\mathcal{G}_\varepsilon^{R(A)}(\boldsymbol{p})$ have a rainbow-like structure (the self-consistent Bonn approximation). Their sum gives $\mathrm{Im}\Sigma_\varepsilon^{R(A)}(\boldsymbol{p}) = \mp\frac{1}{2\tau}$. (The real part is unimportant and ignored.) To calculate the microscopic expression of $\boldsymbol{\phi}_j$, we multiply Eqs. (8) and (9) by the matrix elements of $\boldsymbol{\sigma}$, sum up spin and momentum indices, and subtract the two equations obtained thereby. With the substitution of the following expansion

$$\sum_{\boldsymbol{p}'}\phi_{\alpha\beta,\beta\alpha'}^{\boldsymbol{pp}'} = -\frac{1}{2\pi i\nu}(\delta\mathcal{G}_\varepsilon(\boldsymbol{p}))_{\alpha\alpha'}\phi_0 + \frac{1}{\pi\nu\tau}(\mathcal{G}_{\varepsilon_+}^R(\boldsymbol{p}_+)\boldsymbol{\sigma}\mathcal{G}_{\varepsilon_-}^A(\boldsymbol{p}_-))_{\alpha\alpha'}\cdot\boldsymbol{\phi}_j, \quad (12)$$

we obtain (the group velocity is ≈ 1 for $m/\varepsilon \ll 1$)

$$\boldsymbol{\phi}_j(\boldsymbol{q},\omega) = -i\boldsymbol{q}D(\omega)\phi_0(\boldsymbol{q},\omega),\ D(\omega) = \frac{1}{-i\omega+\gamma(\omega)}, \quad (13)$$

and the microscopic expression of $\gamma(\omega)$:

$$\gamma(\omega) = \frac{1}{\tau}\Bigg(1 - \frac{1}{\pi\nu\tau}\sum_{\boldsymbol{p},\boldsymbol{p}'}(\mathcal{G}_{\varepsilon_-}^A(\boldsymbol{p})\hat{\boldsymbol{q}}\cdot\boldsymbol{\sigma}\mathcal{G}_{\varepsilon_+}^R(\boldsymbol{p}))_{\alpha'\alpha} \times U_{\alpha\beta,\beta'\alpha'}^{\boldsymbol{pp}'}(\boldsymbol{q},\omega)(\mathcal{G}_{\varepsilon_+}^R(\boldsymbol{p}')\hat{\boldsymbol{q}}\cdot\boldsymbol{\sigma}\mathcal{G}_{\varepsilon_-}^A(\boldsymbol{p}'))_{\beta\beta'}\Bigg). \quad (14)$$

Equation (14) implies that τ is renormalized and the ω dependence implies a retarded effect. Substituting Eq. (13) into Eq. (10) gives

$$\phi_0(\boldsymbol{q},\omega) = \frac{i\nu}{-i\omega + D(\omega)\boldsymbol{q}^2}. \quad (15)$$

It shows that ϕ_0 has a diffusive pole. Physically, it implies that a number density fluctuation excited locally relaxes according to a diffusion-like equation. It differs from the normal diffusion equation in that the diffusion constant $D(\omega)$, as shown by its microscopic expression Eqs. (13) and (14), depends generally on ω. (In principle, it also depends on $\boldsymbol{q}$, but this plays no role for $\boldsymbol{q}\to 0$ in this work.) Such dependence accounts for the memory recovery developed in the course of propagation. Whenever $D(\omega)$ is independent of ω and the length scale L, the normal diffusion equation and thus Eq. (1) follows.

As a simple application of the general theory, we ignore the second term in Eq. (14), obtaining $\gamma = \frac{1}{\tau}$. So $D(\omega) = \tau \equiv D_0$ for $\omega \ll \gamma$. This result can also be derived by summing up all the ladder diagrams of ϕ_0, and the sum is thus called "diffuson". Alternatively, it can be obtained by generalizing the Boltzmann kinetic theory developed for spinless disordered Hamiltonians [11,12].

However, this result cannot be extended to arbitrarily small ω or equivalently arbitrarily large L, for which we need to consider diagrams beyond the first order in U_0 and, in particular, those giving rise to singular contributions to U. Let us sum up the maximally crossing diagrams shown in Fig. 2(c), obtaining: $U_{\alpha\beta,\beta'\alpha'}^{\boldsymbol{pp}'} = \frac{\pi\nu U_0^2}{-i\omega+\tau_m^{-1}+D_0(\boldsymbol{p}+\boldsymbol{p}')^2}\Psi_{\alpha\beta'}^0(\Psi^0)_{\beta\alpha'}^* \equiv C_{\alpha\beta,\beta'\alpha'}^{\boldsymbol{p}+\boldsymbol{p}'}(\omega)$. In the presence of the $\hat{T}$ symmetry, $m=0$ and τ_m^{-1} vanishes. So C has a diffusive pole: It is singular at $\boldsymbol{p}\approx -\boldsymbol{p}'$, i.e., $\boldsymbol{Q}\equiv\boldsymbol{p}+\boldsymbol{p}'\approx 0$, and is called "cooperon". When the symmetry is broken, τ_m is finite, which was observed in Ref. [32] and may be regarded as the lifetime of the cooperon. Here Ψ^0 is a projector. $\Psi_{\alpha\beta'}^0$ implies that the spins with indices α, β' form a singlet pair, and so does $(\Psi^0)_{\beta\alpha'}^*$. In principle, there are triplet contributions to U; however, for $\varepsilon/m \gg 1$ they do not display any singularities and can be ignored. With the substitution of U into Eq. (14), we obtain the leading quantum correction to D_0, denoted as δD_1:

$$\frac{\delta D_1}{D_0} = \frac{1}{\pi\nu}\int_{Q<\frac{1}{\tau}}\frac{d\boldsymbol{Q}}{(2\pi)^2}\frac{1}{-i\omega+\tau_m^{-1}+D_0\boldsymbol{Q}^2}. \quad (16)$$

It holds for $|\frac{\delta D_1}{D_0}| \ll 1$, i.e., $\tau\max(\omega,\tau_m^{-1}) \gg e^{-4\pi^2\nu D_0}$. Provided $\omega\tau_m \ll 1$ and $L \gg \sqrt{D_0\tau_m}$, δD_1 is independent of ω, L and reduces to the first line of Eq. (3), giving rise to the weak quantum diffusion. Due to $\nu D_0 = \frac{\varepsilon\tau}{2\pi}$ the inequality $\frac{\tau}{\tau_m} \gg e^{-4\pi^2\nu D_0}$ gives the condition in the introduction that defines the regime I. Equation (16) differs from the well-known weak antilocalization [30] in the appearance of τ_m^{-1}.

For smaller τ_m^{-1}, namely, smaller ω or larger L, we need to go beyond the perturbative cooperon contributions. To perform such a nonperturbative analysis we note that, similar to the spinless case [7], the most singular contributions to U have the diagrammatical structure as shown in Fig. 2(b). There, two singlet cooperons cross an arbitrary diagram (e.g. an infinite series of cooperons) denoted as Z. This gives an expression for the dominant Bethe-Salpeter kernel:

$$U_{\alpha\beta,\beta'\alpha'}^{\boldsymbol{pp}'} \xrightarrow{\text{dominant}} C_{\alpha\beta,\beta'\alpha'}^{\boldsymbol{p}+\boldsymbol{p}'}(\omega) + C_{\alpha\tau,\beta'\rho'}^{\boldsymbol{p}+\boldsymbol{p}'}(\omega)Z_{\tau\rho,\rho'\tau'}^{\boldsymbol{p}+\boldsymbol{p}'}(\omega)C_{\rho\beta,\tau'\alpha'}^{\boldsymbol{p}+\boldsymbol{p}'}(\omega). \quad (17)$$

For $m=0$ it has been shown [27] that $\Psi_{\beta'\alpha}^0 U_{\alpha\beta,\beta'\alpha'}^{\boldsymbol{pp}'}\Psi_{\alpha'\beta}^0 = i\pi U_0^2\phi_0(\boldsymbol{p}+\boldsymbol{p}',\omega)$ with ϕ_0 given by Eq. (15). Intuitively, this identity reflects a reciprocal relation resulting from the $\hat{T}$ symmetry, i.e., when the lower particle line in Fig. 2(b) is rotated so that it goes in the same direction as the upper particle line, the diagrams representing the right-hand side of Eq. (17) are converted into those representing $U_0^2\phi_0(\boldsymbol{p}+\boldsymbol{p}',\omega)$. For $m \ll \varepsilon$ the $\hat{T}$ symmetry is broken only weakly. As a result, the reciprocal relation remains valid, except that similar to the difference between the diffuson and the cooperon, the symmetry breaking term τ_m^{-1} is added to the diffusive pole carried by dominant U. Taking this into account, we obtain

$$U_{\alpha\beta,\beta'\alpha'}^{\boldsymbol{pp}'} \xrightarrow{\text{dominant}} \frac{\pi\nu U_0^2}{-i\omega+\tau_m^{-1}+D(\omega)(\boldsymbol{p}+\boldsymbol{p}')^2}\Psi_{\alpha\beta'}^0(\Psi^0)_{\beta\alpha'}^*. \quad (18)$$

Substituting it into Eqs. (13) and (14) gives

$$\frac{D_0}{D(\omega)} = 1 - \frac{1}{\pi\nu}\int_{Q<\frac{1}{\tau}}\frac{d\boldsymbol{Q}}{(2\pi)^2}\frac{1}{-i\omega+\tau_m^{-1}+D(\omega)\boldsymbol{Q}^2}. \quad (19)$$

This result differs crucially from the self-consistent equation, that describes localization when the breaking of time-reversal symmetry is weak, in the sign of the second term [6]. It cannot be obtained by the nonperturbative field theory for massive Dirac fermions [35] where all cooperon contributions vanish. For low frequencies $\omega\tau_m \ll 1$ one may ignore the ω term. So

$D(\omega)$ is independent of ω, but depends on the length scale L in general. Solving the equation numerically we obtain Fig. 1. We see that as L increases the low-frequency $D(\omega)$ increases from D_0, and levels off at a value, which gives the quantum diffusion constant D. To find an analytic form of the latter, we note that for $L \gg \sqrt{D\tau_m}$ Eq. (19) reduces to Eq. (2). From Eq. (2) we reproduce for the regime I the first line of Eq. (3); this was obtained before from Eq. (16), which is perturbative and corresponds to replacing $D(\omega)$ on the right-hand side of Eq. (19) by D_0. Most importantly, from Eq. (2) we see that $D \gg D_0$ in the regime II; in this case solving Eq. (2) up to the logarithmic accuracy, we obtain the second line of Eq. (3).

IV. INTERPLAY WITH LOCALIZATION

Consider a path representing a quantum amplitude, which moves diffusively at length scale of $\sqrt{D\tau_m}$. Suppose that during this diffusive motion the path self-intersects twice with two loops formed. Then, another quantum amplitude can pass the two loops in different order, and pass each loop along the same direction as the former amplitude. These two paths have the same phase and thus constructively interfere with each other. They give an interference correction to D (not D_0), denoted as δD_2, which is immune to even strong $\hat{T}$-symmetry breaking and cannot be described by the theory developed above. It can be calculated by the field-theoretical approach [17], which is $\frac{\delta D_2}{D} = -\frac{1}{2\pi^2(\nu D)^2} \ln \frac{L}{\sqrt{D\tau_m}}$, a unitary-class weak localization correction to D. δD_2 and D are comparable for $L \sim \sqrt{D\tau_m} e^{2\pi^2(\nu D)^2}$, where the quantum diffusion crosses over to the unitary-class localization. Our findings thus show neither the scaling law for various sympletic class systems [27–29,31] nor that for unitary class systems [31] applies to the present system. It is even not clear to us whether some generalization of the well-known single parameter scaling theory of Anderson localization [37] may exist, since the present system is in the crossover from the sympletic to the unitary class.

V. IMPLICATIONS FOR TOPOLOGICAL INSULATORS

Our findings imply an exotic quantum transport phenomenon in topological insulators. Consider a 3D topological insulator on the substrate of a ferromagnet. The surface electronic states of the topological insulator are described by the 2D massive Dirac equation, with the mass term arising from the Zeeman splitting. Then, by the Einstein relation, the second line of Eq. (3) implies that at zero temperature, as the sample size increases, the surface electron conductance increases from the Drude value and levels off at a value larger than the Drude conductance, as shown in Fig. 1. Finally, we note that the exchange interaction between electrons can give rise to an Altshuler-Aronov type correction [10], which might not be negligible in real experiments on topological insulators [38]. We leave the interplay between such kind of interaction corrections and presently found quantum diffusion for future studies.

ACKNOWLEDGMENTS

Support by Hong Kong Research Grant Council Projects 16307114, 16300818, and by National Natural Science Foundation China Projects 11925507, 12047503, is acknowledged. We wish to thank Yayu Wang for helpful discussions.

[1] *Fifty Years of Anderson Localization*, edited by E. Abrahams (World Scientific, Singapore, 2010).

[2] P. Sheng, *Introduction to Wave Scattering, Localization, and Mesoscopic Phenomena*, 2nd ed. (Springer, Berlin, 2006).

[3] G. Casati, B. V. Chirikov, J. Ford, and F. M. Izrailev, in *Stochastic Behavior in Classical and Quantum Hamiltonian Systems*, edited by G. Casati and J. Ford, Lecture Notes in Physics Vol. 93 (Springer, Berlin, 1979), pp. 334.

[4] S. Fishman, D. R. Grempel, and R. E. Prange, Phys. Rev. Lett. **49**, 509 (1982).

[5] L. P. Gor'kov, A. I. Larkin, and D. E. Khmelnitskii, Pis'ma Zh. Eksp. Teor. Fiz. **30**, 248 (1979) [JETP Lett. **30**, 228 (1979)].

[6] D. Vollhardt and P. Wölfle, Phys. Rev. B **22**, 4666 (1980).

[7] D. Vollhardt and P. Wölfle, in *Electronic Phase Transitions*, edited by W. Hanke and Yu. V. Kopaev (North-Holland, Amsterdam, 1992), pp. 1–78.

[8] C. Tian, A. Kamenev, and A. I. Larkin, Phys. Rev. Lett. **93**, 124101 (2004).

[9] C. Hainaut, P. Fang, A. Rançon, J.-F. Clément, P. Szriftgiser, J.-C. Garreau, C. Tian, and R. Chicireanu, Phys. Rev. Lett. **121**, 134101 (2018).

[10] B. L. Altshuler and A. G. Aronov, Zh. Eksp. Teor. Fiz. **77**, 2028 (1979) [Sov. Phys.—JETP **50**, 968 (1979)].

[11] L. Erdös, M. Salmhofer and H.-T. Yau, in *Mathematical Physics of Quantum Mechanics: Selected and Refereed Lectures from QMath9*, edited by J. Asch and A. Joye, Lecture Notes in Physics Vol. 690 (Springer, Heidelberg, 2006), pp. 233–258.

[12] L. Erdös, M. Salmhofer, and H.-T. Yau, Commun. Math. Phys. **271**, 1 (2007).

[13] T. Dittrich and P. Hänggi, G.-L. Ingold, B. Kramer, G. Schön, and W. Zwerger, *Quantum Transport and Dissipation* (Wiley-VCH, Weinheim, Germany, 1998).

[14] A. Kapitulnik, S. A. Kivelson, and B. Spivak, Rev. Mod. Phys. **91**, 011002 (2019).

[15] C. Yang, Y. Liu, Y. Wang, L. Feng, Q. He, J. Sun, Y. Tang, C. Wu, J. Xiong, W. Zhang *et al.*, Science **366**, 1505 (2019).

[16] Y. Chen and C. Tian, Phys. Rev. Lett. **113**, 216802 (2014).

[17] C. Tian, Y. Chen, and J. Wang, Phys. Rev. B **93**, 075403 (2016).

[18] I. Guarneri, C. Tian, and J. Wang, Phys. Rev. B **102**, 045433 (2020).

[19] I. A. Ado, I. A. Dmitriev, P. M. Ostrovsky, and M. Titov, Europhys. Lett. **111**, 37004 (2015).

[20] N. A. Sinitsyn, J. E. Hill, H. Min, J. Sinova, and A. H. MacDonald, Phys. Rev. Lett. **97**, 106804 (2006).

[21] H.-Z. Lu, J. Shi, and S.-Q. Shen, Phys. Rev. Lett. **107**, 076801 (2011).

[22] M. Z. Hasan and C. L. Kane, Rev. Mod. Phys. **82**, 3045 (2010).

[23] X. L. Qi and S. C. Zhang, Rev. Mod. Phys. **83**, 1057 (2011).

[24] S. Das Sarma, S. Adam, E. H. Hwang, and E. Rossi, Rev. Mod. Phys. **83**, 407 (2011).

[25] S. Hershfield and V. Ambegaokar, Phys. Rev. B **34**, 2147 (1986).

[26] J. Rammer and H. Smith, Rev. Mod. Phys. **58**, 323 (1986).

[27] C. Tian, Phys. Rev. B **86**, 121304(R) (2012).

[28] K. Nomura, M. Koshino, and S. Ryu, Phys. Rev. Lett. **99**, 146806 (2007).

[29] J. H. Bardarson, J. Tworzydlo, P. W. Brouwer, and C. W. J. Beenakker, Phys. Rev. Lett. **99**, 106801 (2007).

[30] S. Hikami, A. I. Larkin, and Y. Nagaoka, Prog. Theor. Phys. **63**, 707 (1980).

[31] K. B. Efetov, *Supersymmetry in Disorder and Chaos* (Cambridge University Press, Cambridge, 1997).

[32] G. Tkachov, *Topological insulators—The Physics of Spin Helicity in Quantum Transport* (Pan Stanford Publishing, Singapore, 2016).

[33] I. V. Gornyi, V. Yu. Kachorovskii, and P. M. Ostrovsky, Phys. Rev. B **90**, 085401 (2014).

[34] See Supplemental Material at http://link.aps.org/supplemental/10.1103/PhysRevB.104.075427 for the complete analytical theory and detailed derivations of the results.

[35] P. M. Ostrovsky, I. V. Gornyi, and A. D. Mirlin, Phys. Rev. Lett. **98**, 256801 (2007).

[36] H. T. Nieh, P. Sheng, and X. B. Wang, Phys. Lett. A **246**, 542 (1998).

[37] E. Abrahams, P. W. Anderson, D. C. Licciardello, and T. V. Ramakrishnan, Phys. Rev. Lett. **42**, 673 (1979).

[38] M. Liu, C.-Z. Chang, Z. Zhang, Y. Zhang, W. Ruan, K. He, L.-L. Wang, X. Chen, J.-F. Jia, S.-C. Zhang *et al.*, Phys. Rev. B **83**, 165440 (2011).

Supplemental materials for
Quantum diffusion of massive Dirac fermions induced by symmetry breaking

Ting Zhang,[1,2], Chushun Tian,[3*], and Ping Sheng[1,2]
[1] Department of Physics, Hong Kong University of Science and Technology, Clear Water Bay, Kowloon, Hong Kong, China
[2] Institute for Advanced Study, Hong Kong University of Science and Technology, Clear Water Bay, Kowloon, Hong Kong, China and
[3] CAS Key Laboratory of Theoretical Physics and Institute of Theoretical Physics, Chinese Academy of Sciences, Beijing 100190, China

This supplementary material (SM) aims at substantially expanding the theory outlined in the main text and explaining in details the derivations of the results presented there. For the convenience of readers this SM is written in a self-contained manner, so that readers need not to resort to the main text. In particular, all the notations are reintroduced and all the results presented in the main text are presented here in a coherent way.

It is in order to expose some motivations of developing a nonperturbative diagrammatic theory for wave propagation of Dirac particles with a small mass in disordered environments. First of all, because it is a two-dimensional (2D) system and the time-reversal symmetry is broken in the presence of finite mass, in the limit of infinite size and infinite time the particle-wave is strongly localized. As we will see in Sec. 4, this localization is of unitary type and occurs in an extremely large scale--practically inaccessible. So, a natural question is: what happens to wave propagation before strong localization sets in?

To address this issue, it is necessary to have a theory that allows us to study not only one-loop perturbative but also nonperturbative effects, for even strong localization does not set in, we have to deal with large length and time scales. The field theories [1, 2], though capable of describing strong local-ization of unitary type, require the time-reversal symme-try to be strongly broken and thus cannot be applied to the present study (see Sec. 4 for more details). On the other hand, the widely adopted diagrammatic method has been developed so far only for treating one-loop perturbative effects such as weak antilocalization, when the mass of Dirac particle does not vanish [3, 4]. In fact, even for Dirac particles with vanishing mass, to develop a nonperturbative theory for their motion in a disordered environment is challenging. In Ref. [2], it was argued based on field theory that the β-function describing the scaling behavior of conductance has two critical points. This result was disproved by numerical exper-iments [5, 6]. Instead, numerical experiments showed that, irrespective of disorder strength, the β-function is as simple as Eq.(S86) below and no phase transition follows, unlike ordinary spin-orbit coupling systems with time-reversal symmetry [1, 7]. The scaling law observed numerically was analytically derived in Ref. [8] by a nonperturbative diagrammatic method developed in that work. Therefore, it is natural to generalize that method to the present system.

This SM is organized as follows. In Sec. 1, we describe the system in details and discuss its symmetry. In Sec. 2, we develop the general theory for the density response of disordered massive Dirac fermions in 2D. We show that the wave propagation follows a generalized diffusion equation, where the diffusion coefficient is frequency dependent. In Sec. 3, we calculate the frequency-dependent diffusion coefficient both perturbatively and nonperturbatively. In the former case, we reproduce the well-known weak antilocalization correction to the Boltzmann diffusion coefficient. In the latter case, we find that due to the weak time-reversal symmetry breaking by a small mass, a normal diffusive wave propagation results, but the diffusion coefficient is larger than that given by the Boltzmann kinetic theory, and grows unboundedly as the energy-to-mass ratio increases. In Sec. 4, we discuss the interplay between the quantum (normal) diffusion and Anderson localization. Some additional technical details are given in Appendices A and B.

1. THE MODEL AND ITS SYMMETRY

We consider Dirac fermions of mass m in the presence of scalar disorders. The propagation of such Dirac fermions is described by

$$\partial_t \psi = \hat{H}\psi, \tag{S1}$$

$$\hat{H} \equiv \boldsymbol{\sigma}\cdot\boldsymbol{p} + m\sigma^z + V(\boldsymbol{r}), \tag{S2}$$

where ψ is a two-component spinor, $\boldsymbol{\sigma} \equiv (\sigma^x, \sigma^y)$ with $\sigma^{x,y,z}$ are the Pauli matrices, and $\boldsymbol{p} \equiv -i\bigtriangledown$, $\boldsymbol{r}$ are the momentum and the position operator, respectively. Both the Fermi velocity and the Plank constant are set to unity throughout this SM. The mass is considered to be very small compared to the particle energy ε throughout this SM. The disorder potential $V(\boldsymbol{r})$ is Gaussian. It has zero mean everywhere, and its fluctuations are spatially independent, $\langle V(\boldsymbol{r})V(\boldsymbol{r}')\rangle = U_0\delta(\boldsymbol{r}-\boldsymbol{r}')$. Here $\langle\cdot\rangle$ denotes the average over disorder configurations, $U_0 = 1/(\pi\nu\tau)$ is the disorder strength, ν is the density of states at ε, and

τ is the characteristic time which, as we will see below, is the elastic scattering time of the order of the Boltzmann collision time. The parameters U_0, ε, m are renormalized at short scales. When such renormalization effects are taken into account they enter into the large-scale physics merely as new parameters [9]. Thus we shall not discuss this further. We focus on the case where $\varepsilon/m \gg 1$ and $\varepsilon\tau \gg 1$.

Define the time-reversal operator $\hat{T} := -i\sigma^y \hat{C}$, where $\hat{C}$ denotes the complex conjugate. For m=0 we have:

$$\hat{T}\hat{H}\hat{T}^{-1} = \hat{H}. \tag{S3}$$

So in this case the time-reversal symmetry is preserved, and the system belongs to the symplectic class according to the random matrix theory [10]. For $m \neq 0$,

$$\hat{T}\hat{H}\hat{T}^{-1} \neq \hat{H}. \tag{S4}$$

So the time-reversal symmetry is broken, and the system belongs to the unitary class. For $m \ll \varepsilon$, the time-reversal symmetry is only weakly broken. This property has important consequences on wave propagation, as we will show below.

2. THE DENSITY RESPONSE THEORY

To study the physics of wave propagation below we generalize the density response theory of 2D massless Dirac fermions, developed by one of us previously [8], to the massive case. From the technical viewpoint, the present theory is in spirit parallel to the well-known Vollhardt-Wölfle theory [11, 12] of strong Anderson localization of spinless particles. However, as we have described in the paper and will show in details below, the physical results are conceptually different from those in that theory.

To start, we introduce the retarded (advanced) Green's function:

$$G_\varepsilon^{R(A)} := 1/(\varepsilon - \hat{H} \pm i\delta), \tag{S5}$$

with δ being a positive infinitesimal. The motion of Dirac Fermions in large length and time scales can be described by the response function defined as:

$$\sum_{\boldsymbol{p},\boldsymbol{p}',\boldsymbol{q}} e^{i(\boldsymbol{p}_+\cdot\boldsymbol{r}_+ - \boldsymbol{p}'_+\cdot\boldsymbol{r}'_+ + \boldsymbol{p}'_-\cdot\boldsymbol{r}'_- - \boldsymbol{p}_-\cdot\boldsymbol{r}_-)} \phi^{\boldsymbol{p}\boldsymbol{p}'}_{\alpha\beta,\beta'\alpha'}(\boldsymbol{q},\omega)$$
$$:= -\frac{1}{2\pi i}\left\langle (G^R_{\varepsilon_+}(\boldsymbol{r}_+,\boldsymbol{r}'_+))_{\alpha\beta}(G^A_{\varepsilon_-}(\boldsymbol{r}'_-,\boldsymbol{r}_-))_{\beta'\alpha'}\right\rangle, \tag{S6}$$

in which $\boldsymbol{p}_\pm = \boldsymbol{p} \pm \frac{\boldsymbol{q}}{2}$, $\boldsymbol{p}'_\pm = \boldsymbol{p}' \pm \frac{\boldsymbol{q}}{2}$, $\varepsilon_\pm = \varepsilon \pm \frac{\omega}{2}$, and $\alpha, \beta, \cdots$ are spin indices. Throughout this SM the Einstein summation convention applies to spin indices. With the disorder average performed, the spatial translational invariance is restored. So only three independent space coordinates: $\frac{\boldsymbol{r}_+ + \boldsymbol{r}_-}{2} - \frac{\boldsymbol{r}'_+ + \boldsymbol{r}'_-}{2}$, $\boldsymbol{r}_+ - \boldsymbol{r}_-$, and $\boldsymbol{r}'_- - \boldsymbol{r}'_+$ appear. They correspond respectively to the Fourier wavenumber $\boldsymbol{q}, \boldsymbol{p}, \boldsymbol{p}'$.

When we expand $G_\varepsilon^{R(A)}$ in V and perform the disorder averaging, each term of $\phi^{\boldsymbol{p}\boldsymbol{p}'}_{\alpha\beta,\beta'\alpha'}$ can be represented by a specific diagram. As shown in Fig. 2(a) in the main text, the backbone of each diagram consists of two particle lines: the upper (lower) particle line corresponds to $G^{R(A)}$. The building blocks of each diagram are the disorder-averaged retarded (advanced) Green's functions $\mathcal{G}_\varepsilon^{R(A)}(\boldsymbol{r}-\boldsymbol{r}') := \langle G^{R(A)}(\boldsymbol{r},\boldsymbol{r}')\rangle$, represented by a solid line going rightwards (leftwards), and the disorder scattering $U_0\delta(\boldsymbol{r}-\boldsymbol{r}')$ is represented by a dashed line. In the Fourier representation $\mathcal{G}_\varepsilon^{R(A)}$ takes the general form:

$$\mathcal{G}_\varepsilon^{R(A)}(\boldsymbol{p}) = (\varepsilon - \boldsymbol{\sigma}\cdot\boldsymbol{p} - m\sigma^z - \Sigma_\varepsilon^{R(A)}(\boldsymbol{p}))^{-1}, \tag{S7}$$

where $\Sigma_\varepsilon^{R(A)}$ is the self-energy. All diagrams of the response function can be organized in the way shown by Fig. 2(a) in the main text, which is described by the Bethe-Salpeter equation:

$$\phi^{\boldsymbol{p}\boldsymbol{p}'}_{\alpha\beta,\beta'\alpha'}(\boldsymbol{q},\omega) = (\mathcal{G}^R_{\varepsilon_+}(\boldsymbol{p}_+))_{\alpha\gamma}(\mathcal{G}^A_{\varepsilon_-}(\boldsymbol{p}_-))_{\gamma'\alpha'}$$
$$\times\Big(-\frac{\delta_{\boldsymbol{p}\boldsymbol{p}'}\delta_{\gamma\beta}\delta_{\beta'\gamma'}}{2\pi i} + \sum_{\boldsymbol{k}} U^{\boldsymbol{p}\boldsymbol{k}}_{\gamma\delta,\delta'\gamma'}(\boldsymbol{q},\omega)\phi^{\boldsymbol{k}\boldsymbol{p}'}_{\delta\beta,\beta'\delta'}(\boldsymbol{q},\omega)\Big), \tag{S8}$$

with $U^{\boldsymbol{p}\boldsymbol{k}}_{\gamma\delta,\delta'\gamma'}(\boldsymbol{q},\omega)$ being the irreducible two-particle interaction vertex function. Each diagram of U has ends joined by the disorder scattering lines, and cannot be separated into disconnected parts by cutting a pair of upper/lower particle line simultaneously, i.e. is two-particle irreducible.

Adopting the method in [13, 14], in the Appendix A we show that U obeys the following Vollhardt-Wölfle type Ward identity, namely, Eq. (7) in the main text:

$$\sum_{\boldsymbol{p}} (\delta\mathcal{G}_\varepsilon(\boldsymbol{p}))_{\gamma'\gamma} U^{\boldsymbol{p}\boldsymbol{k}}_{\gamma\delta,\delta'\gamma'} = (\delta\Sigma_\varepsilon(\boldsymbol{k}))_{\delta'\delta}, \tag{S9}$$

with $\delta\mathcal{G}_\varepsilon(\boldsymbol{p}) := \mathcal{G}^R_{\varepsilon+}(\boldsymbol{p}_+) - \mathcal{G}^A_{\varepsilon-}(\boldsymbol{p}_-)$, and $\delta\Sigma_\varepsilon(\boldsymbol{p}) := \Sigma^R_{\varepsilon+}(\boldsymbol{p}_+) - \Sigma^A_{\varepsilon-}(\boldsymbol{p}_-)$.

Multiplying both sides of Eq. (S8) by $(\mathcal{G}^R_\varepsilon(\boldsymbol{p}_+))^{-1}$, we obtain:

$$(\varepsilon_+ - \boldsymbol{\sigma}\cdot\boldsymbol{p}_+ - m\sigma^z - \Sigma^R_{\varepsilon_+}(\boldsymbol{p}_+))_{\gamma\alpha}\phi^{\boldsymbol{p}\boldsymbol{p}'}_{\alpha\beta,\beta'\alpha'} =$$
$$(\mathcal{G}^A_{\varepsilon_-}(\boldsymbol{p}_-))_{\gamma'\alpha'}\Big(-\frac{\delta_{\boldsymbol{p}\boldsymbol{p}'}\delta_{\gamma\beta}\delta_{\beta'\gamma'}}{2\pi i} + \sum_{\boldsymbol{k}} U^{\boldsymbol{p}\boldsymbol{k}}_{\gamma\delta,\delta'\gamma'}\phi^{\boldsymbol{k}\boldsymbol{p}'}_{\delta\beta,\beta'\delta'}\Big). \tag{S10}$$

Similarly, we have:

$$(\varepsilon_- - \boldsymbol{\sigma}\cdot\boldsymbol{p}_- - m\sigma^z - \Sigma^A_{\varepsilon_-}(\boldsymbol{p}_-))_{\alpha'\gamma'}\phi^{\boldsymbol{p}\boldsymbol{p}'}_{\alpha\beta,\beta'\alpha'} =$$
$$(\mathcal{G}^R_{\varepsilon_+}(\boldsymbol{p}_+))_{\alpha\gamma}\Big(-\frac{\delta_{\boldsymbol{p}\boldsymbol{p}'}\delta_{\gamma\beta}\delta_{\beta'\gamma'}}{2\pi i} + \sum_{\boldsymbol{k}} U^{\boldsymbol{p}\boldsymbol{k}}_{\gamma\delta,\delta'\gamma'}\phi^{\boldsymbol{k}\boldsymbol{p}'}_{\delta\beta,\beta'\delta'}\Big). \tag{S11}$$

We then set $\beta = \beta'$ in both equations, set $\gamma = \alpha'$ in Eq. (S10), and set $\gamma' = \alpha$ in Eq. (S11), and sum up the spin indices. By further subtracting the ensuing two equations, we obtain:

$$\begin{aligned}&\Big(\omega - \boldsymbol{\sigma}\cdot\boldsymbol{q} - \delta\Sigma_\varepsilon(\boldsymbol{p})\Big)_{\alpha'\alpha}\phi^{\boldsymbol{p}\boldsymbol{p}'}_{\alpha\beta,\beta\alpha'}(\boldsymbol{q},\omega)\\ =&\frac{(\delta\mathcal{G}_\varepsilon(\boldsymbol{p}))_{\beta\beta}}{2\pi i} - \sum_{\boldsymbol{k}}(\delta\mathcal{G}_\varepsilon(\boldsymbol{p}))_{\alpha\gamma}U^{\boldsymbol{p}\boldsymbol{k}}_{\gamma\delta,\delta'\alpha}(\boldsymbol{q},\omega)\phi^{\boldsymbol{k}\boldsymbol{p}'}_{\delta\beta,\beta\delta'}(\boldsymbol{q},\omega).\end{aligned} \tag{S12}$$

With the help of the Ward identity Eq. (S9), upon summing up the momenta $\boldsymbol{p}$, $\boldsymbol{p}'$ we obtain:

$$-i\omega\phi_0(\boldsymbol{q},\omega) + i\boldsymbol{q}\cdot\boldsymbol{\phi}_j(\boldsymbol{q},\omega) = i\nu, \tag{S13}$$

which describes the particle number conservation macroscopically. Here $\nu(\varepsilon) = \frac{1}{2\pi i}\sum_{\boldsymbol{p}}(\mathcal{G}^A_\varepsilon(\boldsymbol{p}) - \mathcal{G}^R_\varepsilon(\boldsymbol{p}))_{\alpha\alpha}$ is the density of states, ϕ_0 and $\boldsymbol{\phi}_j$ are the density relaxation function and the current relaxation function, respectively, whose microscopic expressions are:

$$\phi_0 = \sum_{\boldsymbol{p},\boldsymbol{p}'}\phi^{\boldsymbol{p}\boldsymbol{p}'}_{\alpha\beta,\beta\alpha}, \tag{S14}$$

$$\boldsymbol{\phi}_j = \sum_{\boldsymbol{p},\boldsymbol{p}'}\boldsymbol{\sigma}_{\alpha'\alpha}\phi^{\boldsymbol{p}\boldsymbol{p}'}_{\alpha\beta,\beta\alpha'}. \tag{S15}$$

Equation (S13) relates ϕ_0 and $\boldsymbol{\phi}_j$. Physically, Eqs. (S13)-(S15) that follow from Eqs. (S10) and (S11) are in spirit similar to that hydrodynamic equations follow from the Boltzmann kinetic equation, and Eq. (S13) is exact, irrespective of the disorder strength.

Similar to the usual hydrodynamical theory, if another relation between ϕ_0 and $\boldsymbol{\phi}_j$ exists, then the equation set for ϕ_0 and $\boldsymbol{\phi}_j$ is closed and can be solved. Below we show that for $\varepsilon\tau \gg 1$, such an equation exists. In this limit we can employ the self-consistent Born approximation to find the self-energy of Green's function, which satisfies:

$$\Sigma^{R(A)}_\varepsilon = U_0\int\frac{d\boldsymbol{k}}{(2\pi)^2}\frac{1}{\varepsilon - \boldsymbol{\sigma}\cdot\boldsymbol{k} - m\sigma^z - \Sigma^{R(A)}_\varepsilon}. \tag{S16}$$

Thus we have:

$$\mathrm{Im}\Sigma^{R(A)}_\varepsilon(\boldsymbol{p}) = \mp\frac{1}{2\tau} \tag{S17}$$

for $m/\varepsilon \ll 1$. The real part of the self-energy is unimportant and we shall not discuss it further.

To proceed further, we expand $\sum_{\boldsymbol{p}'}\phi^{\boldsymbol{p}\boldsymbol{p}'}_{\alpha\beta,\beta\alpha'}$ in terms of the moments of the microscopic current $\boldsymbol{\sigma}\phi_0$ and $\boldsymbol{\phi}_j$. More precisely, we have the following general form:

$$\sum_{\boldsymbol{p}'}\phi^{\boldsymbol{p}\boldsymbol{p}'}_{\alpha\beta,\beta\alpha'} = (a_0(\boldsymbol{p}))_{\alpha\alpha'}\phi_0 + (\boldsymbol{a}(\boldsymbol{p}))_{\alpha\alpha'}\cdot\boldsymbol{\phi}_j, \tag{S18}$$

where the coefficients a_0 and $\boldsymbol{a}$ are to be determined. Because $\delta\mathcal{G}_\varepsilon(\boldsymbol{p})$ is strongly peaked at the Fermi momentum for $\varepsilon\tau \gg 1$, the $\boldsymbol{p}$-dependence of the left-hand side is dominated by this structure carried by $\delta\mathcal{G}_\varepsilon(\boldsymbol{p})$. So, a_0 must be proportional to $\delta\mathcal{G}_\varepsilon(\boldsymbol{p})$. The proportionality coefficient can be found by setting $\alpha = \alpha'$, summing up α, and requiring both sides thereby obtained to be equal. As a result,

$$a_0 = -\frac{\delta\mathcal{G}_\varepsilon(\boldsymbol{p})}{2\pi i\nu}. \tag{S19}$$

Then, by taking into account this structure and that $\boldsymbol{a}$ is proportional to the microscopic current $\boldsymbol{\sigma}$, we find that $\boldsymbol{a}$ is proportional to $\mathcal{G}^R_{\varepsilon_+}(\boldsymbol{p}_+)\boldsymbol{\sigma}\mathcal{G}^A_{\varepsilon_-}(\boldsymbol{p}_-)$. The proportionality coefficient can be determined by multiplying both sides of Eq. (S18) by $\boldsymbol{\sigma}_{\alpha'\alpha}$, summing up the spin indices, and requiring both sides thereby obtained to be equal. As a result,

$$\boldsymbol{a} = \frac{\mathcal{G}^R_{\varepsilon_+}(\boldsymbol{p}_+)\boldsymbol{\sigma}\mathcal{G}^A_{\varepsilon_-}(\boldsymbol{p}_-)}{\pi\nu\tau}. \tag{S20}$$

Substituting Eqs. (S19) and (S20) into Eq. (S18), we obtain:

$$\begin{aligned}\sum_{\boldsymbol{p}'}\phi^{\boldsymbol{p}\boldsymbol{p}'}_{\alpha\beta,\beta\alpha'} =& -\frac{1}{2\pi i\nu}(\delta\mathcal{G}_\varepsilon(\boldsymbol{p}))_{\alpha\alpha'}\phi_0\\ &+\frac{1}{\pi\nu\tau}(\mathcal{G}^R_{\varepsilon_+}(\boldsymbol{p}_+)\boldsymbol{\sigma}\mathcal{G}^A_{\varepsilon_-}(\boldsymbol{p}_-))_{\alpha\alpha'}\cdot\boldsymbol{\phi}_j,\end{aligned} \tag{S21}$$

namely, the Eq. (12) in the main text.

We are now ready to find another relation between $\boldsymbol{\phi}_j$ and ϕ_0. Noting that the considered Dirac system is isotropic, we have:

$$\boldsymbol{\phi}_j(\boldsymbol{q},\omega) = \phi_j(q,\omega)\hat{\boldsymbol{q}}, \tag{S22}$$

where $\hat{\boldsymbol{q}} = \boldsymbol{q}/q$ is the unit vector in the $\boldsymbol{q}$ direction, and $\phi_j(q,\omega)$ is the module of the vector $\boldsymbol{\phi}_j(\boldsymbol{q},\omega)$. Combining this with Eq. (S15), we obtain:

$$\phi_j(q,\omega) = \sum_{\boldsymbol{p},\boldsymbol{p}'}\hat{\boldsymbol{q}}\cdot\boldsymbol{\sigma}_{\alpha'\alpha}\phi^{\boldsymbol{p}\boldsymbol{p}'}_{\alpha\beta,\beta\alpha'}(\boldsymbol{q},\omega). \tag{S23}$$

To calculate the right-hand side we multiply both sides of Eq. (S10) by $\hat{\boldsymbol{q}}\cdot\boldsymbol{\sigma}_{\alpha'\gamma}$, let $\beta = \beta'$, and sum up all spin indices and momenta. As a result:

$$
\begin{aligned}
&\varepsilon_+\phi_j - \sum_{\boldsymbol{p},\boldsymbol{p}'}(\hat{\boldsymbol{q}}\cdot\boldsymbol{p}_+ + i\sigma^z(\hat{\boldsymbol{q}}\times\boldsymbol{p}_+) - im\hat{\boldsymbol{q}}\times\boldsymbol{\sigma} + \hat{\boldsymbol{q}}\cdot\boldsymbol{\sigma}\Sigma^R_{\varepsilon+}(\boldsymbol{p}_+))_{\alpha'\alpha}\phi^{\boldsymbol{p}\boldsymbol{p}'}_{\alpha\beta,\beta\alpha'}\\
&= -\frac{1}{2\pi i}\sum_{\boldsymbol{p}}(\hat{\boldsymbol{q}}\cdot\boldsymbol{\sigma}\mathcal{G}^A_{\varepsilon-}(\boldsymbol{p}_-))_{\alpha'\alpha'} + \sum_{\boldsymbol{p},\boldsymbol{p}',\boldsymbol{k}}(\mathcal{G}^A_{\varepsilon-}(\boldsymbol{p}-)\hat{\boldsymbol{q}}\cdot\boldsymbol{\sigma})_{\gamma'\gamma}U^{\boldsymbol{p}\boldsymbol{k}}_{\gamma\delta,\delta'\gamma'}\phi^{\boldsymbol{k}\boldsymbol{p}'}_{\delta\beta,\beta\delta'}.
\end{aligned}
\tag{S24}
$$

Likewise, from Eq. (S11) we obtain:

$$
\begin{aligned}
&\varepsilon_-\phi_j - \sum_{\boldsymbol{p},\boldsymbol{p}'}(\hat{\boldsymbol{q}}\cdot\boldsymbol{p}_- - i\sigma^z(\hat{\boldsymbol{q}}\times\boldsymbol{p}_-) + im\hat{\boldsymbol{q}}\times\boldsymbol{\sigma} + \Sigma^A_{\varepsilon-}(\boldsymbol{p}_-)\hat{\boldsymbol{q}}\cdot\boldsymbol{\sigma})_{\alpha'\alpha}\phi^{\boldsymbol{p}\boldsymbol{p}'}_{\alpha\beta,\beta\alpha'}\\
&= -\frac{1}{2\pi i}\sum_{\boldsymbol{p}}(\hat{\boldsymbol{q}}\cdot\boldsymbol{\sigma}\mathcal{G}^R_{\varepsilon+}(\boldsymbol{p}_+))_{\gamma\gamma} + \sum_{\boldsymbol{p},\boldsymbol{p}',\boldsymbol{k}}(\hat{\boldsymbol{q}}\cdot\boldsymbol{\sigma}\mathcal{G}^R_{\varepsilon+}(\boldsymbol{p}_+))_{\gamma'\gamma}U^{\boldsymbol{p}\boldsymbol{k}}_{\gamma\delta,\delta'\gamma'}\phi^{\boldsymbol{k}\boldsymbol{p}'}_{\delta\beta,\beta\delta'}.
\end{aligned}
\tag{S25}
$$

Subtracting Eq. (S25) from Eq. (S24), we obtain:

$$
\begin{aligned}
\left(\omega+\frac{i}{\tau}\right)\phi_j - q\phi_0 =& 2i\sum_{\boldsymbol{p},\boldsymbol{p}'}(\sigma^z(\hat{\boldsymbol{q}}\times\boldsymbol{p}) - m\hat{\boldsymbol{q}}\times\boldsymbol{\sigma})_{\alpha'\alpha}\phi^{\boldsymbol{p}\boldsymbol{p}'}_{\alpha\beta,\beta\alpha'} + \frac{1}{2\pi i}\sum_{\boldsymbol{p}}(\hat{\boldsymbol{q}}\cdot\boldsymbol{\sigma}(\mathcal{G}^R_{\varepsilon+}(\boldsymbol{p}_+) - \mathcal{G}^A_{\varepsilon-}(\boldsymbol{p}-)))_{\alpha'\alpha'}\\
&+\sum_{\boldsymbol{p},\boldsymbol{p}',\boldsymbol{k}}(\mathcal{G}^A_{\varepsilon-}(\boldsymbol{p}_-)(\hat{\boldsymbol{q}}\cdot\boldsymbol{\sigma}(\mathcal{G}^R_{\varepsilon+}(\boldsymbol{p}_+))^{-1} - (\mathcal{G}^A_{\varepsilon-}(\boldsymbol{p}_-))^{-1}\hat{\boldsymbol{q}}\cdot\boldsymbol{\sigma})\mathcal{G}^R_{\varepsilon+}(\boldsymbol{p}_+))_{\gamma'\gamma}U^{\boldsymbol{p}\boldsymbol{k}}_{\gamma\delta,\delta'\gamma'}\phi^{\boldsymbol{k}\boldsymbol{p}'}_{\delta\beta,\beta\delta'},
\end{aligned}
\tag{S26}
$$

where to obtain the $\frac{i}{\tau}\phi_j$ term we have used the fact of:

$$
\mathcal{G}^{R,A}_{\varepsilon}(\boldsymbol{p}) = \frac{\hat{P}}{\varepsilon - \sqrt{p^2+m^2} \pm \frac{i}{2\tau}}, \qquad \hat{P} = \frac{1}{2} + \frac{1}{2}\frac{\boldsymbol{\sigma}\cdot\boldsymbol{p} + m\sigma^z}{\sqrt{p^2+m^2}},
\tag{S27}
$$

for $\varepsilon\tau \gg 1$. Substituting Eq. (S21) into the first two terms on the right-hand side of Eq. (S26), with the help of Eq. (S27) we find that both of them vanish. So Eq. (S26) is simplified to:

$$
\left(\omega+\frac{i}{\tau}\right)\phi_j - q\phi_0 = \sum_{\boldsymbol{p},\boldsymbol{p}',\boldsymbol{k}}\Big(\mathcal{G}^A_{\varepsilon-}(\boldsymbol{p}_-)(\hat{\boldsymbol{q}}\cdot\boldsymbol{\sigma}(\mathcal{G}^R_{\varepsilon+}(\boldsymbol{p}_+))^{-1} - (\mathcal{G}^A_{\varepsilon-}(\boldsymbol{p}_-))^{-1}\hat{\boldsymbol{q}}\cdot\boldsymbol{\sigma})\mathcal{G}^R_{\varepsilon+}(\boldsymbol{p}_+)\Big)_{\gamma'\gamma}U^{\boldsymbol{p}\boldsymbol{k}}_{\gamma\delta,\delta'\gamma'}\phi^{\boldsymbol{k}\boldsymbol{p}'}_{\delta\beta,\beta\delta'}.
\tag{S28}
$$

Thanks to

$$
\hat{\boldsymbol{q}}\cdot\boldsymbol{\sigma}(\mathcal{G}^R_{\varepsilon+}(\boldsymbol{p}_+))^{-1} - (\mathcal{G}^A_{\varepsilon-}(\boldsymbol{p}_-))^{-1}\hat{\boldsymbol{q}}\cdot\boldsymbol{\sigma} = \left(\omega+\frac{i}{\tau}\right)\hat{\boldsymbol{q}}\cdot\boldsymbol{\sigma} - q - 2i\sigma^z\hat{\boldsymbol{q}}\times\boldsymbol{p} + 2im\hat{\boldsymbol{q}}\times\boldsymbol{\sigma}
\tag{S29}
$$

and

$$
\phi_j(q,\omega) = \int\frac{d\varphi_{\hat{\boldsymbol{q}}}}{2\pi}\phi_j(q,\omega),
\tag{S30}
$$

where $\varphi_{\hat{\boldsymbol{q}}}$ is the angle corresponding to the direction of $\hat{\boldsymbol{q}}$, upon substituting Eqs. (S21) and (S29) into Eq. (S28), and performing the angular average of Eq. (S30), we find that the contribution arising from the first term of Eq. (S21) to the right-hand side of Eq. (S29) vanishes ($\omega, q \ll \frac{1}{\tau}$). Furthermore, because $\boldsymbol{\sigma}\cdot\hat{\boldsymbol{q}}$ is the microscopic current in the $\hat{\boldsymbol{q}}$ direction, for the contribution to the right-hand side of Eq. (S29) arising from the second term of Eq. (S21), one needs to take only the $\frac{i}{\tau}\hat{\boldsymbol{q}}\cdot\boldsymbol{\sigma}$ term into account for that the others do not contribute. So Eq (S28) is reduced to

$$
\left(\omega+\frac{i}{\tau}\left(1-\frac{1}{\pi\nu\tau}\sum_{\boldsymbol{p},\boldsymbol{p}'}(\mathcal{G}^A_{\varepsilon-}(\boldsymbol{p}_-)\hat{\boldsymbol{q}}\cdot\boldsymbol{\sigma}\mathcal{G}^R_{\varepsilon+}(\boldsymbol{p}_+))_{\alpha'\alpha}U^{\boldsymbol{p}\boldsymbol{p}'}_{\alpha\beta,\beta'\alpha'}(\mathcal{G}^R_{\varepsilon+}(\boldsymbol{p}'_+)\hat{\boldsymbol{q}}\cdot\boldsymbol{\sigma}\mathcal{G}^A_{\varepsilon-}(\boldsymbol{p}'_-))_{\beta\beta'}\right)\right)\phi_j = q\phi_0.
\tag{S31}
$$

Combining Eqs. (S22) and (S31), we have:

$$
\boldsymbol{\phi}_j(\boldsymbol{q},\omega) = -i\boldsymbol{q}D(\omega)\phi_0(\boldsymbol{q},\omega),
\tag{S32}
$$

where

$$D(\omega) = \frac{1}{-i\omega + \gamma(\omega)}, \tag{S33}$$

with

$$\gamma(\omega) = \frac{1}{\tau}\left(1 - \frac{1}{\pi\nu\tau}\sum_{\boldsymbol{p},\boldsymbol{p}'}(\mathcal{G}^A_{\varepsilon_-}(\boldsymbol{p}_-)\hat{\boldsymbol{q}}\cdot\boldsymbol{\sigma}\mathcal{G}^R_{\varepsilon_+}(\boldsymbol{p}_+))_{\alpha'\alpha}U^{\boldsymbol{p}\boldsymbol{p}'}_{\alpha\beta,\beta'\alpha'}(\boldsymbol{q},\omega)(\mathcal{G}^R_{\varepsilon_+}(\boldsymbol{p}'_+)\hat{\boldsymbol{q}}\cdot\boldsymbol{\sigma}\mathcal{G}^A_{\varepsilon_-}(\boldsymbol{p}'_-))_{\beta\beta'}\right). \tag{S34}$$

With Eqs. (S13) and (S33), the density relaxation function ϕ_0 and the current relaxation function $\boldsymbol{\phi}_j$ are solved:

$$\phi_0(\boldsymbol{q},\omega) = \frac{i\nu}{-i\omega + D(\omega)q^2}, \tag{S35}$$

$$\boldsymbol{\phi}_j(\boldsymbol{q},\omega) = \frac{\nu D(\omega)\boldsymbol{q}}{-i\omega + D(\omega)q^2}. \tag{S36}$$

We see that ϕ_0 has a diffusive pole. Physically this implies that a number density fluctuation excited locally relaxes according to a diffusive-like equation. The diffusion coefficient $D(\omega)$ depends on ω, which accounts for the memory recovery developed in the course of propagation. In principle, it also depends on $\boldsymbol{q}$, but in our work $\boldsymbol{q}\to 0$. Note that when D is ω independent, the normal diffusion equation is recovered.

3. THE FREQUENCY-DEPENDENT DIFFUSION COEFFICIENT $D(\omega)$

When the second term in Eq. (S34) is ignored, $\gamma = 1/\tau$ and thus $D(\omega) = \tau \equiv D_0$, which is ω independent (for $\omega\tau \ll 1$). This result can also be derived by summing up all the particle (namely, the upper particle line)-hole (namely, the lower particle line) ladder diagrams of ϕ_0, and the sum is thus called diffuson. Alternatively, it can be obtained by generalizing the Boltzmann kinetic theory developed for spinless disordered Hamiltonians [15, 16]. For these reasons, we may call D_0 the Boltzmann diffusion constant. It is well known that D_0 excludes all wave interference effects. In this section we will apply the general theory to the second term of Eq. (S34), and we will especially focus on its behaviors at low frequencies. This will allow us to find both the perturbative and nonperturbative effects of wave interference.

3.1 Weak antilocalization

To calculate the second term in Eq. (S34), we seek for the diagrammatical structures that give singular contributions to $U^{\boldsymbol{p}\boldsymbol{p}'}_{\alpha\beta,\beta'\alpha'}$. In this subsection we investigate contributions that arise from the maximally crossing diagrams, which are denoted as $(\Lambda_0^{\boldsymbol{p}\boldsymbol{p}'}(\boldsymbol{q},\omega))_{\alpha\beta,\beta'\alpha'}$. These diagrams differ from those presented in Fig. 2(c) in the main text in that the spin indices $\alpha,\beta,\alpha',\beta'$ can be arbitrary. Note that the diagram composed of single disorder scattering line is included as well.

Passing to the Fourier representation, we have:

$$\left(\Lambda_0^{\boldsymbol{p}\boldsymbol{p}'}\right)_{\alpha\beta,\beta'\alpha'} = U_0\delta_{\alpha\beta}\delta_{\alpha'\beta'} + U_0\sum_{\boldsymbol{k}}\left(\mathcal{G}^R_{\varepsilon+}(\boldsymbol{k})\right)_{\alpha\gamma}\left(\mathcal{G}^A_{\varepsilon-}(\boldsymbol{p}+\boldsymbol{p}'-\boldsymbol{k})\right)_{\beta'\gamma'}\left(\Lambda_0^{\boldsymbol{k}(\boldsymbol{p}+\boldsymbol{p}'-\boldsymbol{k})}\right)_{\gamma\beta,\gamma'\alpha'}. \tag{S37}$$

This implies that Λ_0 depends on $\boldsymbol{p},\boldsymbol{p}'$ via $\boldsymbol{p}+\boldsymbol{p}'$, i.e.

$$\left(\Lambda_0^{\boldsymbol{p}\boldsymbol{p}'}(\boldsymbol{q},\omega)\right)_{\alpha\beta,\beta'\alpha'} \equiv \left(\Lambda_0^{\boldsymbol{Q}}(\omega)\right)_{\alpha\beta,\beta'\alpha'}, \qquad \boldsymbol{Q} = \boldsymbol{p}+\boldsymbol{p}'. \tag{S38}$$

To proceed we introduce a characteristic time:

$$\tilde{\tau} := \frac{\tau}{1+(\frac{m}{\varepsilon})^2} \tag{S39}$$

and the rescaling:

$$\left(\Lambda_0^{\boldsymbol{Q}}(\omega)\right)_{\alpha\beta,\beta'\alpha'} \to \frac{U_0\tau}{\tilde{\tau}^2}\left(\Lambda_0^{\boldsymbol{Q}}(\omega)\right)_{\alpha\beta,\beta'\alpha'} \tag{S40}$$

to rewrite Eq. (S37) as

$$\left(\Lambda_0^{\boldsymbol{Q}}(\omega)\right)_{\alpha\beta,\beta'\alpha'} = \frac{\tilde{\tau}^2}{\tau}\delta_{\alpha\beta}\delta_{\alpha'\beta'} + U_0\sum_{\boldsymbol{k}}\left(\mathcal{G}^R_{\varepsilon+}(\boldsymbol{k})\right)_{\alpha\gamma}\left(\mathcal{G}^A_{\varepsilon-}(\boldsymbol{Q}-\boldsymbol{k})\right)_{\beta'\gamma'}\left(\Lambda_0^{\boldsymbol{Q}}(\omega)\right)_{\gamma\beta,\gamma'\alpha'}. \tag{S41}$$

It is standard [3] to expand Λ_0 in the spin singlet and triplet basis,

$$\left(\Lambda_0^{\boldsymbol{Q}}(\omega)\right)_{\alpha\beta,\beta'\alpha'} = \sum_{i,j=0,x,y,z}\Psi^i_{\alpha\beta'}\Psi^{j*}_{\beta\alpha'}C^{ij}(\boldsymbol{Q},\omega), \qquad \Psi^i := \frac{\tau^i\tau^y}{\sqrt{2}}, \tag{S42}$$

where $i(j)=0$ stands for the singlet component and $i(j)=x,y,z$ for the triplet components, with $\Psi^{i(j)}$ being the corresponding projectors. These singlet and triplet states are formed by pairing one spin in the end of the upper particle line with the other in the end of the lower particle line [cf. Fig. 2(c) in the main text], and the Pauli matrices τ^i $(i=0,x,y,z)$ are defined on the corresponding sector. With the substitution of Eq. (S42) into Eq. (S41) and using Eq. (S27), we obtain:

$$-\left(\overline{e_x}-i\overline{e_ye_\perp}\right)C^{00} + \left(\frac{\tau}{\tilde{\tau}} - \left(\overline{e_\perp^2}+\overline{e_x^2}\right)\right)C^{x0} - \left(\overline{e_xe_y}-i\overline{e_\perp}\right)C^{y0} = 0, \tag{S43}$$

$$-\left(\overline{e_y}+i\overline{e_xe_\perp}\right)C^{00} - \left(\overline{e_xe_y}+i\overline{e_\perp}\right)C^{x0} + \left(\frac{\tau}{\tilde{\tau}} - \left(\overline{e_\perp^2}+\overline{e_y^2}\right)\right)C^{y0} = 0, \tag{S44}$$

$$\left(\frac{\tau}{\tilde{\tau}} - \left(\overline{e_x^2}+\overline{e_y^2}\right)\right)C^{00} - \left(\overline{e_x}+i\overline{e_ye_\perp}\right)C^{x0} - \left(\overline{e_y}-i\overline{e_xe_\perp}\right)C^{y0} = \tilde{\tau}, \tag{S45}$$

where

$$e_\perp = \frac{m}{\sqrt{\boldsymbol{p}^2+m^2}}, \qquad e_x = \frac{p_x}{\sqrt{\boldsymbol{p}^2+m^2}}, \qquad e_y = \frac{p_y}{\sqrt{\boldsymbol{p}^2+m^2}}, \tag{S46}$$

and

$$\overline{\cdots} := \int\frac{d\varphi_{\hat{\boldsymbol{Q}}}}{2\pi}(...)\frac{1}{1-i\omega\tilde{\tau}+i\tilde{\tau}\hat{\boldsymbol{p}}\cdot\boldsymbol{Q}}, \tag{S47}$$

with $\hat{\boldsymbol{p}}$ being the unit vector along the direction of the particle momentum $\boldsymbol{p}$.

From Eqs. (S43) and (S44), we obtain:

$$C^{x0} = \frac{\left(\frac{\tau}{\tilde{\tau}} - (\overline{e_\perp^2}+\overline{e_y^2})\right)\left(\overline{e_x}-i\overline{e_ye_\perp}\right) + \left(\overline{e_xe_y}-i\overline{e_\perp}\right)\left(\overline{e_y}+i\overline{e_xe_\perp}\right)}{\left(\frac{\tau}{\tilde{\tau}} - (\overline{e_\perp^2}+\overline{e_y^2})\right)\left(\frac{\tau}{\tilde{\tau}} - (\overline{e_\perp^2}+\overline{e_x^2})\right) - \left(\overline{e_xe_y}-i\overline{e_\perp}\right)\left(\overline{e_xe_y}+i\overline{e_\perp}\right)}C^{00}, \tag{S48}$$

and

$$C^{y0} = \frac{(\overline{e_ye_x}+i\overline{e_\perp})(\overline{e_x}-i\overline{e_\perp e_y}) + \left(\frac{\tau}{\tilde{\tau}} - (\overline{e_\perp^2}+\overline{e_x^2})\right)\left(\overline{e_y}+i\overline{e_xe_\perp}\right)}{\left(\frac{\tau}{\tilde{\tau}} - (\overline{e_\perp^2}+\overline{e_x^2})\right)\left(\frac{\tau}{\tilde{\tau}} - (\overline{e_\perp^2}+\overline{e_y^2})\right) - (\overline{e_xe_y}-i\overline{e_\perp})(\overline{e_xe_y}+i\overline{e_\perp})}C^{00}. \tag{S49}$$

In the limit $\boldsymbol{Q}\to 0$, Eqs. (S48) and (S49) reduce to:

$$C^{x0} = -2i\tilde{\tau}\frac{1}{e_\parallel^3}\left((1-\frac{1}{2}e_\parallel^2)(Q_x-ie_\perp Q_y) - ie_\perp(Q_y+ie_\perp Q_x)\right)C^{00}, \tag{S50}$$

and

$$C^{y0} = -2i\tilde{\tau}\frac{1}{e_\parallel^3}\left((1-\frac{1}{2}e_\parallel^2)(Q_y+ie_\perp Q_x) + ie_\perp(Q_x-ie_\perp Q_y)\right)C^{00}, \tag{S51}$$

where $e_\parallel = \sqrt{1-e_\perp^2}$. Substituting Eqs. (S50) and (S51) into Eq. (S45), we obtain:

$$C^{00} = \frac{1}{e_\parallel^2}\frac{1}{\frac{2e_\perp^2}{e_\parallel^2\tilde{\tau}} - i\omega + \tilde{\tau}Q^2(1+\frac{4e_\perp^2}{e_\parallel^4})}. \tag{S52}$$

For $m \ll \varepsilon$, it is simplified to:

$$C^{00} = \frac{1}{\tau_m^{-1} - i\omega + D_0 Q^2}, \tag{S53}$$

with

$$\tau_m = \left(\frac{\varepsilon}{m}\right)^2 \frac{\tau}{2}. \tag{S54}$$

Finally, undoing the rescaling Eq. (S40) gives

$$C^{00} = \frac{\pi\nu U_0^2}{\tau_m^{-1} - i\omega + D_0 Q^2} \equiv C^{\boldsymbol{Q}}(\omega). \tag{S55}$$

For $m = 0$ and thus vanishing τ_m^{-1}, the system bears the $\hat{T}$-symmetry. In this case, C^{00} is singular at $\boldsymbol{Q} = \boldsymbol{p}+\boldsymbol{p}' = 0$ and $\omega = 0$. For $m \neq 0$, the symmetry is broken and the system belongs to the unitary class. In this case, a finite τ_m results. Therefore, we see that for $m \ll \varepsilon$, the most singular contributions to $(\Lambda_0^{\boldsymbol{Q}})_{\alpha\beta,\beta'\alpha'}$ arise from the cooperon component with $i = j = 0$, dubbed the singlet cooperon. Therefore, the spin states (α, β') must be paired into a spin-singlet and so do (β, α'), as shown by Fig. 2(c) in the main text. So in Eq. (S42) we keep only the $i = j = 0$ component. With the further substitution of Eq. (S55) we find the corresponding singular contributions to U, which is:

$$\frac{\pi\nu U_0^2}{-i\omega + \tau_m^{-1} + D_0 Q^2} \Psi^0_{\alpha\beta'} (\Psi^0)^*_{\beta\alpha'} =: C^{\boldsymbol{Q}}_{\alpha\beta,\beta'\alpha'}(\omega). \tag{S56}$$

Substituting it into Eq. (S34) gives:

$$\begin{aligned}\gamma(\omega) =& \frac{1}{\tau}\Big(1 - \frac{1}{\pi\nu\tau} \sum_{\boldsymbol{p},\boldsymbol{Q}} (\mathcal{G}^A_{\varepsilon_-}(\boldsymbol{p}) \hat{\boldsymbol{q}} \cdot \boldsymbol{\sigma} \mathcal{G}^R_{\varepsilon_+}(\boldsymbol{p}))_{\alpha'\alpha} \\ &\times \frac{\pi\nu U_0^2}{-i\omega + \tau_m^{-1} + D_0 Q^2} \frac{\tau^y_{\alpha\beta'}}{\sqrt{2}} \frac{-\tau^y_{\beta\alpha'}}{\sqrt{2}} \\ &\times (\mathcal{G}^R_{\varepsilon_+}(-\boldsymbol{p}) \hat{\boldsymbol{q}} \cdot \boldsymbol{\sigma} \mathcal{G}^A_{\varepsilon_-}(-\boldsymbol{p}))_{\beta\beta'}\Big).\end{aligned} \tag{S57}$$

With the $\boldsymbol{p}$ sum performed, we obtain:

$$\gamma(\omega) = \frac{1}{\tau}\left(1 - \frac{1}{\pi\nu}\int \frac{d\boldsymbol{Q}}{(2\pi)^2} \frac{1}{-i\omega + \tau_m^{-1} + D_0 Q^2}\right), \tag{S58}$$

which gives

$$\frac{\delta D}{D_0} = \frac{1}{\pi\nu}\int_{Q<\frac{1}{\tau}} \frac{d\boldsymbol{Q}}{(2\pi)^2} \frac{1}{-i\omega + \tau_m^{-1} + D_0 Q^2}. \tag{S59}$$

When τ_m^{-1} vanishes this reproduces the well-known weak antilocalization correction to the Boltzmann diffusion constant [3, 7]. Equation (S59) is essentially a one-loop perturbative result. It does not apply for extremely large length scale L and extremely small ω, i.e. in the nonperturbative regime. We are not aware of any methods that allow us to go beyond the one-loop perturbation theory for nonvanishing but small τ_m^{-1}, i.e. weak $\hat{T}$-symmetry breaking. In fact, for this case the previous diagrammatic theories [3, 4] have been restricted to one loop, while nonperturbative field theories [1, 2] have been developed for systems with $\hat{T}$-symmetry either preserved or strongly broken. As a result, they do not apply here.

3.2 Symmetry breaking-induced diffusion: beyond weak antilocalization

In this subsection we will develop a nonperturbative theory of wave propagation of Dirac particles. We will first consider the massless case and then generalize the results to the massive case with $m/\varepsilon \ll 1$.

3.2.1 Closed equation for $D(\omega)$

We introduce the full vertex function, $\Gamma^{\boldsymbol{p}\boldsymbol{p}'}_{\alpha\beta,\beta'\alpha'}(\boldsymbol{q},\omega)$. As shown in Fig. S1, it is related to $U^{\boldsymbol{p}\boldsymbol{p}'}_{\alpha\beta,\beta'\alpha'}(\boldsymbol{q},\omega)$ via the following Bethe-Salpeter equation:

$$\Gamma^{\boldsymbol{p}\boldsymbol{p}'}_{\alpha\beta,\beta'\alpha'} = U^{\boldsymbol{p}\boldsymbol{p}'}_{\alpha\beta,\beta'\alpha'} + \sum_{\boldsymbol{k}} U^{\boldsymbol{p}\boldsymbol{k}}_{\alpha\delta,\delta'\alpha'} R^{\boldsymbol{k}}_{\delta\gamma,\gamma'\delta'} \Gamma^{\boldsymbol{k}\boldsymbol{p}'}_{\gamma\beta,\beta'\gamma'}, \tag{S60}$$

where

$$R^{\boldsymbol{k}}_{\delta\gamma,\gamma'\delta'}(\boldsymbol{q},\omega) \equiv (\mathcal{G}^R_{\varepsilon+}(\boldsymbol{k}_+))_{\delta\gamma} (\mathcal{G}^A_{\varepsilon-}(\boldsymbol{k}_-))_{\gamma'\delta'} \tag{S61}$$

and the arguments $(\boldsymbol{q},\omega)$ in Γ and U have been suppressed in order to make the formula compact. It is easy to see that Γ can be written as [Fig. S2(a)]

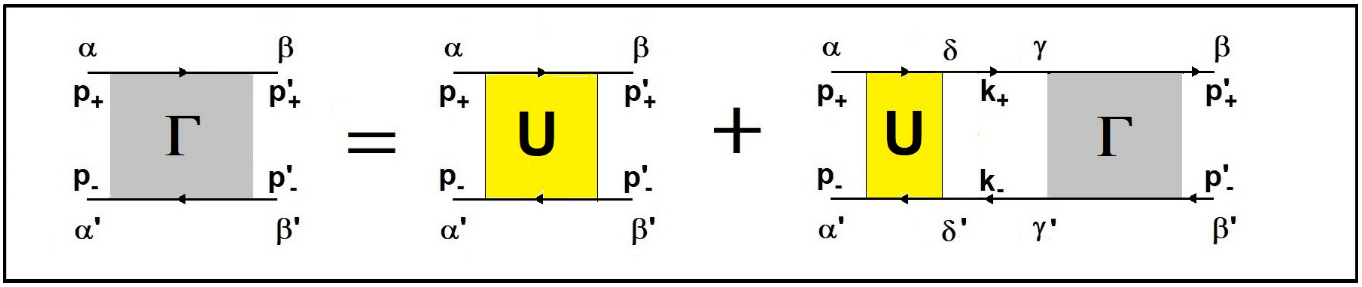

Fig. S1. Diagrammatical representation of Eq. (S60).

$$\Gamma^{\boldsymbol{p}\boldsymbol{p}'}_{\alpha\beta,\beta'\alpha'} = \left(\chi^{\boldsymbol{p}\boldsymbol{p}'} + \Gamma_0^{\boldsymbol{p}\boldsymbol{p}'} + \sum_{\boldsymbol{k}_1}\Gamma_0^{\boldsymbol{p}\boldsymbol{k}_1}R^{\boldsymbol{k}_1}\chi^{\boldsymbol{k}_1\boldsymbol{p}'} + \sum_{\boldsymbol{k}_1}\chi^{\boldsymbol{p}\boldsymbol{k}_1}R^{\boldsymbol{k}_1}\Gamma_0^{\boldsymbol{k}_1\boldsymbol{p}'} + \sum_{\boldsymbol{k}_1,\boldsymbol{k}_2}\Gamma_0^{\boldsymbol{p}\boldsymbol{k}_1}R^{\boldsymbol{k}_1}\chi^{\boldsymbol{k}_1\boldsymbol{k}_2}R^{\boldsymbol{k}_2}\Gamma_0^{\boldsymbol{k}_2\boldsymbol{p}'}\right)_{\alpha\beta,\beta'\alpha'}. \tag{S62}$$

Here χ stands for the sum of all diagrams without a particle-hole ladder on the very left or right, Γ_0 stands for the sum of all particle-hole ladders, and we have defined the product of two general two-particle functions: $A \equiv \{A_{\alpha\beta,\beta'\alpha'}\}$ and $B \equiv \{B_{\alpha\beta,\beta'\alpha'}\}$ as follows:

$$C := AB \quad \Longleftrightarrow \quad C_{\alpha\beta,\beta'\alpha'} := A_{\alpha\delta,\delta'\alpha'}B_{\delta\beta,\beta'\delta'}, \tag{S63}$$

which is readily seen to be associative, i.e.

$$(AB)C = A(BC). \tag{S64}$$

It is easy to show that $\Gamma_0^{\boldsymbol{p}\boldsymbol{p}'}$ has no dependence on $\boldsymbol{p}$, $\boldsymbol{p}'$. So Eq. (S62) can be simplified as

$$\Gamma^{\boldsymbol{p}\boldsymbol{p}'}_{\alpha\beta,\beta'\alpha'} = \left(\chi^{\boldsymbol{p}\boldsymbol{p}'} + \Gamma_0 + \Gamma_0\left(\sum_{\boldsymbol{k}_1}R^{\boldsymbol{k}_1}\chi^{\boldsymbol{k}_1\boldsymbol{p}'}\right) + \left(\sum_{\boldsymbol{k}_1}\chi^{\boldsymbol{p}\boldsymbol{k}_1}R^{\boldsymbol{k}_1}\right)\Gamma_0 + \Gamma_0\left(\sum_{\boldsymbol{k}_1,\boldsymbol{k}_2}R^{\boldsymbol{k}_1}\chi^{\boldsymbol{k}_1\boldsymbol{k}_2}R^{\boldsymbol{k}_2}\right)\Gamma_0\right)_{\alpha\beta,\beta'\alpha'}. \tag{S65}$$

Thanks to $m = 0$, the $\hat{T}$-symmetry follows, giving:

$$\mathcal{G}^A_\varepsilon(\boldsymbol{p}) = (-i\sigma^y)(\mathcal{G}^A_\varepsilon(-\boldsymbol{p}))^T(i\sigma^y), \tag{S66}$$

where T stands for the transpose. Using this relation and noting that $\Gamma^{\boldsymbol{p}\boldsymbol{p}'}_{\alpha\beta,\beta'\alpha'}(\boldsymbol{q},\omega)$ is the full vertex function, we can readily prove the following identity:

$$\begin{aligned}\Gamma^{\boldsymbol{p}\boldsymbol{p}'}_{\alpha\beta,\beta'\alpha'}(\boldsymbol{q},\omega) =& (i\sigma^y)_{\alpha'\alpha''}\Gamma^{\frac{\boldsymbol{p}-\boldsymbol{p}'+\boldsymbol{q}}{2}\,\frac{\boldsymbol{p}'-\boldsymbol{p}+\boldsymbol{q}}{2}}_{\alpha\beta,\alpha''\beta''}(\boldsymbol{p}+\boldsymbol{p}',\omega)(-i\sigma^y)_{\beta''\beta'}\\ =& (-1)^{s(\alpha')+s(\beta')}\Gamma^{\frac{\boldsymbol{p}-\boldsymbol{p}'+\boldsymbol{q}}{2}\,\frac{\boldsymbol{p}'-\boldsymbol{p}+\boldsymbol{q}}{2}}_{\alpha\beta,\overline{\alpha'}\,\overline{\beta'}}(\boldsymbol{p}+\boldsymbol{p}',\omega).\end{aligned} \tag{S67}$$

where the overline over the spin index transforms an up ($\uparrow$)-spin into a down ($\downarrow$)-spin and vice versa, and

$$s(\alpha) := \begin{cases} 0, \alpha = \uparrow; \\ 1, \alpha = \downarrow. \end{cases} \tag{S68}$$

The second line of Eq. (S67) can be diagrammatically represented by Fig. S2(b) with the help of Fig. S2(a). By twisting the lower particle line in Fig. S2(b) and applying Eq. (S66) again, we obtain Fig. S2(c). Note that the factor $(-1)^{s(\alpha')+s(\beta')}$ is multiplied by a new factor $(-1)^{s(\overline{\alpha'})+s(\overline{\beta'})}$, giving $(-1)^{s(\alpha')+s(\beta')}(-1)^{s(\overline{\alpha'})+s(\overline{\beta'})} = (-1)^2 = 1$; thus no factor arises in Fig. S2(c). Recall that the diagrams of Λ_0 are obtained from those of Γ_0 by twisting the lower particle line, which has been analyzed in Sec. 3.1. The similar diagrammatical rule holds for $\overline{\chi}$. However, it should be emphasized that, like the spinless case [12], the propagation direction of the upper and lower particle lines in Fig.

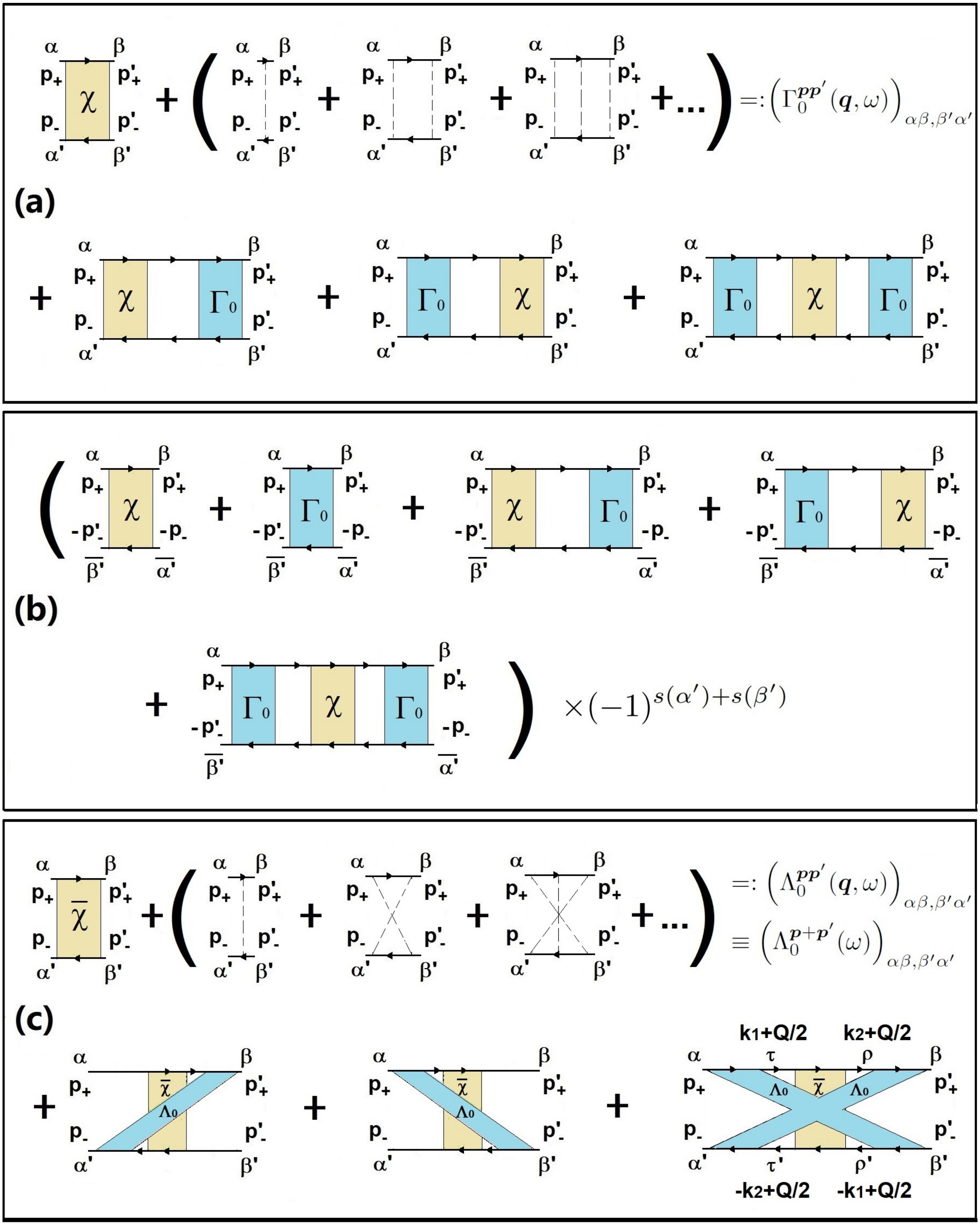

Fig. S2. (a).Diagrammatical representation of $\Gamma^{\boldsymbol{p}\boldsymbol{p}'}_{\alpha\beta,\beta'\alpha'}(\boldsymbol{q},\omega)$; (b) Diagrammatical representation of the second line of Eq. (S67) obtained directly from (a); (c) Equivalent representation of (b).

S2(a) and Fig. S2(c) are the same; moreover, all the external momenta and spin indices in the same places of Fig. S2(a) and Fig. S2(c) are the same.

Note that U is the two-particle irreducible vertex. From Eq. (S60) we find that the diagrams representing U are the last four diagrams of Fig. S2(c) and the irreducible part of $\overline{\chi}$. In Sec. 3.1 we have shown that the $i=j=0$ component of the second diagram in Fig. S2(c), i.e. the singlet cooperon shown in Fig. 2(c) in the main text:

$$C^{\boldsymbol{Q}}_{\alpha\beta,\beta'\alpha'}(\omega)|_{\tau_m^{-1}=0} = \frac{\pi\nu U_0^2}{-i\omega + D_0 Q^2}\Psi^0_{\alpha\beta'}(\Psi^0)^*_{\beta\alpha'} \tag{S69}$$

gives rise to the weak anti-localization. To find other singular contributions to U, which diverge in the infrared limit $\boldsymbol{Q}\to 0$, $\omega\to 0$, likewise we replace Λ_0 in the last three diagrams of Fig. S2(c) by the singlet cooperon in Fig. 2(c) in the main text. On the other hand, it is easy to see that the irreducible part of $\overline{\chi}$ does not suffer infrared divergence. Thus the first diagram in Fig. S2(c) can be ignored. Because the last diagram in Fig. S2(c) includes two singlet cooperons, it must dominate over the second , the third, and the fourth diagrams which includes only one singlet cooperon. Therefore, the dominant contribution to U is

$$U^{\boldsymbol{pp}'}_{\alpha\beta,\beta'\alpha'}(\boldsymbol{q},\omega) \overset{\text{dominant}}{\longrightarrow} C^{\boldsymbol{Q}}_{\alpha\beta,\beta'\alpha'}(\omega) + C^{\boldsymbol{Q}}_{\alpha\tau,\beta'\rho'}(\omega) Z^{\boldsymbol{Q}}_{\tau\rho,\rho'\tau'}(\omega) C^{\boldsymbol{Q}}_{\rho\beta,\tau'\alpha'}(\omega), \tag{S70}$$

where

$$Z^{\boldsymbol{Q}}_{\tau\rho,\rho'\tau'}(\omega) = \sum_{\boldsymbol{k}_1,\boldsymbol{k}_2}\left(R^{\frac{\boldsymbol{k}_1-\boldsymbol{k}_2+\boldsymbol{Q}}{2}}(\boldsymbol{k}_1+\boldsymbol{k}_2,\omega)\overline{\chi}^{\frac{\boldsymbol{k}_1-\boldsymbol{k}_2+\boldsymbol{Q}}{2}\frac{\boldsymbol{k}_2-\boldsymbol{k}_1+\boldsymbol{Q}}{2}}(\boldsymbol{k}_1+\boldsymbol{k}_2,\omega)R^{\frac{\boldsymbol{k}_2-\boldsymbol{k}_1+\boldsymbol{Q}}{2}}(\boldsymbol{k}_1+\boldsymbol{k}_2,\omega)\right)_{\tau\rho,\rho'\tau'} \tag{S71}$$

with the diagrams representing $\overline{\chi}$ obtained from those representing χ through twisting their lower particle lines. Note that in Eq. (S70) $C^{\boldsymbol{Q}}_{\alpha\beta,\beta'\alpha'}(\omega)$ is included so that the leading perturbative quantum corrections obtained in Sec. 3.1 can be recovered. Equation (S70), namely, Eq. (17) in the main text, is diagrammatically represented by Fig. 2(b) in the main text.

To proceed we prove in Appendix B the following identity:

$$U_0^2(-2\pi i)\phi_0(\boldsymbol{q},\omega) = \left(\Gamma_0(\boldsymbol{q},\omega) - U_0 + \Gamma_0(\boldsymbol{q},\omega)\left(\sum_{\boldsymbol{k}_1,\boldsymbol{k}_2} Z^{\boldsymbol{k}_1\boldsymbol{k}_2}(\boldsymbol{q},\omega)\right)\Gamma_0(\boldsymbol{q},\omega)\right)_{\alpha\beta,\beta\alpha}, \tag{S72}$$

where

$$Z^{\boldsymbol{k}_1\boldsymbol{k}_2}_{\alpha\beta,\beta'\alpha'}(\boldsymbol{q},\omega) = \left(R^{\boldsymbol{k}_1}(\boldsymbol{q},\omega)\chi^{\boldsymbol{k}_1\boldsymbol{k}_2}(\boldsymbol{q},\omega)R^{\boldsymbol{k}_2}(\boldsymbol{q},\omega)\right)_{\alpha\beta,\beta'\alpha'}. \tag{S73}$$

Next, we consider the diagram representing $(\Gamma_0^{\boldsymbol{pp}'}(\boldsymbol{q},\omega))_{\alpha\beta,\beta'\alpha'}$ with arbitrary spin indices: $\alpha,\beta,\alpha',\beta'$ [Fig. S3(a)]. By twisting the lower particle line we obtain maximally crossing diagrams [Fig. S3(b)]. By further applying Eq. (S66), we obtain Fig. S3(c). Note that the direction of the lower particle line, as well as its end momenta and spin indicies, is different from that in Fig. S3(b). Because these three diagrams are equivalent, we have:

$$\left(\Gamma_0^{\boldsymbol{pp}'}(\boldsymbol{q},\omega)\right)_{\alpha\beta,\beta'\alpha'} = \left(\Lambda_0^{\frac{\boldsymbol{p}-\boldsymbol{p}'+\boldsymbol{q}}{2}\frac{\boldsymbol{p}'-\boldsymbol{p}+\boldsymbol{q}}{2}}(\boldsymbol{p}+\boldsymbol{p}',\omega)\right)_{\alpha\beta,\overline{\alpha'}\,\overline{\beta'}} \times (-1)^{s(\alpha')+s(\beta')}, \tag{S74}$$

where the diagrammatical definition of Λ_0 [Fig. S2(c)] has been used.

With the help of Eq. (S38), we simplify Eq. (S74) as

$$\left(\Gamma_0^{\boldsymbol{pp}'}(\boldsymbol{q},\omega)\right)_{\alpha\beta,\beta'\alpha'} = (\Lambda_0^{\boldsymbol{q}}(\omega))_{\alpha\beta,\overline{\alpha'}\,\overline{\beta'}} \times (-1)^{s(\alpha')+s(\beta')}. \tag{S75}$$

For $(\Lambda_0^{\boldsymbol{q}})_{\alpha\beta,\overline{\alpha'}\,\overline{\beta'}}$, by analysis in Sec. 3.1, among its 16 components only one diverges in the infrared limit: $\boldsymbol{q},\omega\to 0$, which corresponds to that $(\alpha,\overline{\alpha'})$ are paired into a spin singlet and so are $(\beta,\overline{\beta'})$. So, using Eqs. (S42) and (S55) we find $\Gamma^{\boldsymbol{pp}'}(\boldsymbol{q},\omega)$ in the limit: $\boldsymbol{q},\omega\to 0$, which is

$$\left(\Gamma_0^{\boldsymbol{pp}'}(\boldsymbol{q},\omega)\right)_{\alpha\beta,\beta'\alpha'} \simeq C^{\boldsymbol{q}}(\omega)\Psi^0_{\alpha\overline{\alpha'}}(\Psi^0)^*_{\beta\overline{\beta'}} \times (-1)^{s(\alpha')+s(\beta')} = \frac{\pi\nu U_0^2}{-i\omega+D_0 q^2}\frac{\delta_{\alpha\alpha'}}{\sqrt{2}}\frac{\delta_{\beta\beta'}}{\sqrt{2}}. \tag{S76}$$

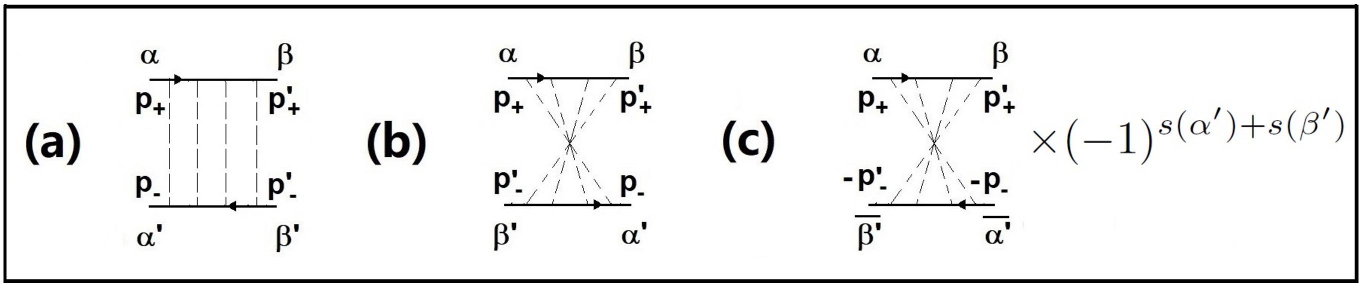

Fig. S3. Diagrammatical proof of Eq. (S74).

[In fact, by directly summing up all the ladder diagrams in Fig. S3(a) it can be shown that this is true also for nonvanishing τ_m^{-1}.] Substituting Eq. (S76) into Eq. (S72) and using Eq. (S35), we obtain:

$$\frac{\pi\nu U_0^2}{-i\omega+D(\omega)q^2}+2U_0=\frac{\pi\nu U_0^2}{-i\omega+D_0q^2}+\left(\frac{\pi\nu U_0^2}{-i\omega+D_0q^2}\right)^2\cdot\frac{1}{2}\sum_{\boldsymbol{k}_1,\boldsymbol{k}_2}Z^{\boldsymbol{k}_1\boldsymbol{k}_2}_{\alpha\beta,\beta\alpha}(\boldsymbol{q},\omega). \tag{S77}$$

On the other hand, we can substitute Eq. (S56) into Eq. (S70), obtaining:

$$U^{\boldsymbol{p}\boldsymbol{p}'}_{\alpha\beta,\beta'\alpha'}(\boldsymbol{q},\omega)\overset{\text{dominant}}{\longrightarrow}\left(\frac{\pi\nu U_0^2}{-i\omega+D_0Q^2}+\left(\frac{\pi\nu U_0^2}{-i\omega+D_0Q^2}\right)^2\Psi^0_{\tau\rho'}Z^{\boldsymbol{Q}}_{\tau\rho,\rho'\tau'}(\omega)(\Psi^0)^*_{\rho\tau'}\right)\Psi^0_{\alpha\beta'}(\Psi^0)^*_{\beta\alpha'}. \tag{S78}$$

To calculate the factor: $\Psi^0_{\tau\rho'}Z^{\boldsymbol{Q}}_{\tau\rho,\rho'\tau'}(\omega)(\Psi^0)^*_{\rho\tau'}$ in the second term of the bracket, we perform an analysis, which is similar to the derivations of Eq. (S74), for Eq. (S71). As a result,

$$Z^{\boldsymbol{Q}}_{\tau\rho,\rho'\tau'}(\omega)=\sum_{\boldsymbol{k}_1,\boldsymbol{k}_2}\left(R^{\boldsymbol{k}_1}(\boldsymbol{Q},\omega)\chi^{\boldsymbol{k}_1\boldsymbol{k}_2}(\boldsymbol{Q},\omega)R^{\boldsymbol{k}_2}(\boldsymbol{Q},\omega)\right)_{\tau\rho,\overline{\tau'}\,\overline{\rho'}}\times(-1)^{s(\tau')+s(\rho')}. \tag{S79}$$

This gives

$$\Psi^0_{\tau\rho'}Z^{\boldsymbol{Q}}_{\tau\rho,\rho'\tau'}(\omega)(\Psi^0)^*_{\rho\tau'}=\frac{1}{2}\sum_{\boldsymbol{k}_1,\boldsymbol{k}_2}Z^{\boldsymbol{k}_1\boldsymbol{k}_2}_{\tau\rho,\rho\tau}(\boldsymbol{Q},\omega). \tag{S80}$$

We then substitute it into Eq. (S78). With the help of Eq. (S77) we reduce Eq. (S78) to

$$U^{\boldsymbol{p}\boldsymbol{p}'}_{\alpha\beta,\beta'\alpha'}(\boldsymbol{q},\omega)\overset{\text{dominant}}{\longrightarrow}\frac{\pi\nu U_0^2}{-i\omega+D(\omega)Q^2}\Psi^0_{\alpha\beta'}(\Psi^0)^*_{\beta\alpha'},\qquad for\quad m=0, \tag{S81}$$

where the unimportant $2U_0$ term has been ignored. This corresponds to Eq. (18) in the main text with $\tau_m^{-1}=0$ and was reported in Ref. [8] without giving the details of the derivations.

For nonvanishing m but $m\ll\varepsilon$, the $\hat{T}$-symmetry is broken but only weakly. Since the diffusive pole arises from the $\hat{T}$-symmetry, we add the symmetry breaking term τ_m^{-1} to the diffusive pole of Eq. (S81) (similar procedures were carried out in the self-consistent theory of Anderson localization [11].) This gives

$$U^{\boldsymbol{p}\boldsymbol{p}'}_{\alpha\beta,\beta'\alpha'}(\boldsymbol{q},\omega)\overset{\text{dominant}}{\longrightarrow}\frac{\pi\nu U_0^2}{-i\omega+\tau_m^{-1}+D(\omega)Q^2}\Psi^0_{\alpha\beta'}(\Psi^0)^*_{\beta\alpha'},\qquad for\quad 0<m\ll\varepsilon. \tag{S82}$$

Substituting it into Eqs. (S33) and (S34), we obtain the following closed equation for $D(\omega)$:

$$\frac{D_0}{D(\omega)}=1-\frac{1}{\pi\nu}\int_{Q<\frac{1}{\tau}}\frac{d\boldsymbol{Q}}{(2\pi)^2}\frac{1}{-i\omega+\tau_m^{-1}+D(\omega)Q^2}, \tag{S83}$$

namely, Eq. (19) in the main text. This result differs crucially from the self-consistent equation, that describes localization when the breaking of time-reversal symmetry is weak, in the sign of the second term. It cannot be obtained by the nonperturbative field theory for massive

Dirac fermions where all cooperon contributions vanish [2]. It is important that Eq. (S83) holds for both strong and weak disorders, i.e. both small and large U_0.

3.2.2 Superdiffusion for $m = 0$

Let us first study Eq. (S83) in the limiting case, i.e. $\tau_m^{-1} = 0$ or $m = 0$, where the $\hat{T}$-symmetry is not broken. For $\omega = 0$, Eq. (S83) can be solved exactly, giving for arbitrarily large length scale L (note that the weak anti-localization applies only for $L \ll \tau e^{2\pi^2\nu D_0}$.):

$$D(0) = D_0 + \frac{1}{2\pi^2\nu}\ln\left(\frac{L}{\tau}\right). \tag{S84}$$

By using Einstein's relation and letting L be the sample size, we obtain the conductance for $L \gg \tau e^{2\pi^2\nu D_0}$, which is

$$g(L) = \frac{e^2}{2\pi^2}\ln\left(\frac{L}{\tau}\right). \tag{S85}$$

This gives:

$$\frac{d\ln g}{d\ln L} = \frac{1}{\pi g} \tag{S86}$$

with g rescaled by $\frac{e^2}{h}$. We emphasize that because this law was obtained from the self-consistent Eq. (S83), it holds even for strong disorders or small g. This was first found in numerical experiments [5, 6], which is contrary to the prediction by arguments based on the field theory [2]. The scaling law Eq. (S86) is a basic characteristic of the topological metal. Indeed, Eq. (S86) has no correc-tions from higher order $1/g$ expansion; it is well known that negative corrections from higher order $1/g$ expansion lead to a fixed point signaling a phase transition. This implies the absence of phase transition in 2D which oc-curs to non-Dirac materials with the $\hat{T}$-symmetry. This fundamental difference might be attributed to the Klein tunneling which is a unique property of Dirac materials and is not carried by usual (i.e. nonrelativistic) spin-orbit coupling systems with $\hat{T}$-symmetry [7]. Indeed, as disorders become stronger and stronger, particles are more and more readily converted into holes of the same energy and *vice versa*. Consequently, strong disorders tend to delocalize, instead of to localize, a particle or a hole. This counterintuitive picture ceases to work for nonrelativistic spin systems, due to the absence of hole states.

To address the issue of wave propagation inside the bulk, we solve Eq. (S83) for low frequencies, $\omega\tau \lesssim e^{-4\pi^2\nu D_0}$, obtaining:

$$D(\omega) \simeq \frac{1}{4\pi^2\nu}\ln\frac{1}{-i\omega\tau}, \quad for \quad \omega\tau \lesssim e^{-4\pi^2\nu D_0}. \tag{S87}$$

from which the wavepacket spreading, characterized by $\langle \boldsymbol{r}^2\rangle_t$, is

$$\begin{aligned}\langle \boldsymbol{r}^2\rangle_t = &\int \frac{d\omega}{2\pi}\frac{1-e^{-i\omega t}}{\omega^2}D(\omega)\\ &\xrightarrow{t\gg\tau e^{4\pi^2\nu D_0}} \frac{t\ln(t/\tau)}{4\pi^2\nu}.\end{aligned} \tag{S88}$$

So the wavepacket spreading is superdiffusive.

3.2.3 Quantum diffusion for small m

For small $m \ll \varepsilon$, $\tau_m^{-1} > 0$, the $\hat{T}$-symmetry is weakly broken. For low frequencies, $\omega\tau_m \ll 1$, the ω term in the denominator of Eq. (S83) can be dropped out. As a result, $D(\omega)$ is ω independent: $D(\omega) = D$, which satisfies

$$\begin{aligned}\frac{D_0}{D} =&1 - \frac{1}{\pi\nu}\int_{Q<\frac{1}{\tau}}\frac{d\boldsymbol{Q}}{(2\pi)^2}\frac{1}{\tau_m^{-1}+DQ^2}\\ =&1 - \frac{1}{2\pi^2\nu}\int_{L^{-1}}^{\tau^{-1}} dQQ\frac{1}{\tau_m^{-1}+DQ^2}.\end{aligned} \tag{S89}$$

From this we see that D may still depend on the length scale L considered in general. To investigate this L-dependence of D we solve Eq. (S89) numerically and the result is shown in Fig. 1 in the main text. We see that it first increases logarithmically with L, and levels off at a quantum value. The latter can be found by setting L^{-1} to zero in Eq. (S89), which gives

$$\frac{D_0}{D} = 1 - \frac{1}{2\pi^2\nu}\int_0^{\tau^{-1}} dQQ\frac{1}{\tau_m^{-1}+DQ^2}, \tag{S90}$$

namely, Eq. (2) in the main text. Equation (S90) can be rewritten as

$$\begin{aligned}D =&D_0 + \frac{1}{4\pi^2\nu}\ln\left(\frac{D}{\tau}\frac{\tau_m}{\tau}+1\right)\\ \simeq&D_0 + \frac{1}{2\pi^2\nu}\ln\frac{\varepsilon}{\sqrt{2}m},\end{aligned} \tag{S91}$$

where in deriving the second line we have used $\varepsilon\tau \gg 1$ and $\tau_m/\tau \gg 1$. For $\frac{\varepsilon}{m} \ll e^{\pi\varepsilon\tau}$ (namely, regime I in the main text), the second term is much smaller than the first. So quantum interference gives a small positive correction to the Boltzmann diffusion constant: this is nothing but the weak antilocalization. For $\frac{\varepsilon}{m} \gg e^{\pi\varepsilon\tau}$ (namely, regime II in the main text), the second term dominates over the first,

$$D = \frac{1}{2\pi^2\nu}\ln\frac{\varepsilon}{\sqrt{2}m}. \tag{S92}$$

This quantum diffusion constant is determined by ν and ε/m, independent of the disorder parameter. With the help of Eq. (S87) we see that Eq. (S92) follows from replacing $\frac{1}{-i\omega}$ in Eq. (S87) by τ_m. Correspondingly, Eq. (S92) gives the diffusive law:

$$\langle \boldsymbol{r}^2 \rangle_t \sim \frac{t}{2\pi^2\nu} \ln \frac{\varepsilon}{\sqrt{2m}} \tag{S93}$$

for wavepacket spreading at sufficiently long (but finite, see Sec. 4 for detailed discussions) time. Comparing Eq. (S93) with Eq. (S88), we find that the quantum diffusive law Eq. (S93) is recovered from the superdiffusive law Eq. (S88) by replacing t in the logarithm of the latter by τ_m. In this sense, we may regard quantum diffusion found here as a remnant of the superdiffusion in topological metals.

A possible physical picture for quantum diffusion is as follows. First of all, when the particle moves in a disordered environment, random scattering by impurities renders the memory of momentum lost at the time scale τ, like in the canonical Einstein-Boltzmann paradigm. However, at longer times the memory gets recovered by constructive interference between different propagating paths of quantum waves. In combination with the helicity, that introduces strong spin-momentum locking, the memory recovery enhances the relaxation time of momentum and renormalizes τ: the more the memory is recovered, the slower the momentum relaxes. Then, as on one hand the quantum interference rests on the $\hat{T}$-symmetry, while on the other hand this symmetry is weakly broken by small m, the constructive interference and the ensuing memory recovery can persist only up to τ_m. After that the particle undergoes random scattering again. So at the time scale of τ_m the wavepacket propagation is diffusive, but with the diffusion constant enhanced from D_0 by the memory recovery.

4. INTERPLAY WITH LOCALIZATION

The nonperturbative results obtained in Sec.3.2.3, though valid for very small frequency ω and very large length scale L, cannot be extended to the limiting case of $\omega = 0$ and L=∞. Indeed, because of the $\hat{T}$-symmetry breaking the system belongs to the unitary class. For this system is 2D and not at the critical point of a quantum Hall transition, it has to exhibit strong localization at the limit of $\omega = 0$ and L=∞. So, a question arises naturally: can localization effects, either strong or weak, originating from the $\hat{T}$-symmetry breaking dominate over the quantum diffusion found in the present work?

To address this problem, let us ignore all quantum diffusion effects for the moment. By using the nonlinear σ-model of unitary type [1], it is easy to show that the leading weak localization correction to D_0 is at the two-loop level (in contrast to the one-loop level — arising from the cooperon — for the orthogonal or sympletic class). Letting this correction be comparable to D_0 gives the localization length:

$$\xi_0 \simeq \tau e^{2\pi^2(\nu D_0)^2}. \tag{S94}$$

It is easy to show that practically [more precisely, for $\frac{\varepsilon}{m} \ll e^{(\varepsilon\tau)^2}/2$], the scale for quantum diffusion to occur, i.e. $\sqrt{D\tau_m}$ is much smaller than ξ_0. As a result, well before the weak localization effect sets in, the quantum diffusion dominates in wave physics, and its effect has to be carried over to localization physics at large time or length scale.

Unfortunately, the σ-model for the unitary class ignores all contributions from the cooperon. Consequently, it cannot describe the quantum diffusion. Now because $\sqrt{D\tau_m}$ is much smaller than ξ_0, one may regard the quantum diffusion as a renormalization of the bare diffusion constant in the σ-model, which is D_0. Upon replacing D_0 in the σ-model by D, we obtain a new localization length formula:

$$\xi \simeq \sqrt{D\tau_m} e^{2\pi^2(\nu D)^2}. \tag{S95}$$

This length is exponentially large at $(\nu D)^2$. Therefore, both weak and strong localization effects can be ignored in practice, and only the quantum diffusion found here is visible.

We remark that because the present system is in the crossover from the sympletic to the unitary class, it is not clear whether the well-known single-parameter scaling theory of Anderson localization [17] may be generalized to the present system. In fact, even for spinless systems, we are not aware of any such single-parameter scaling theory that applies in a regime that crosses over from one symmetry to the other.

APPENDIX A. PROOF OF THE WARD IDENTITY

In this Appendix, we generalize the method of Refs. [13, 14] developed for disordered systems without spin-orbit coupling to disordered massive Dirac fermions, and prove a special type, namely, the Vollhardt-Wölfle type, of Ward identity Eq. (S9). This type of Ward identity for disordered spinless electron systems was first given in Ref. [11] and generalized to more general spinless disordered systems in Refs. [13, 14]. For massless Dirac fermions a Ward identity of this type was given in Ref. [8]. The proof of the Vollhardt-Wölfle type Ward identity developed in Refs. [13, 14] is substantially simpler than that in Ref. [11] and, most importantly, can be more readily generalized to spinful systems. However, how the disorder average introduces the effective statistical interaction in that specific field theoretic setting was not discussed in details in the original papers [13, 14]; this will be given below.

As first noticed in Refs. [13, 14], to derive that special type of Ward identities it is more convenient to adopt the standard many-body technique [18, 19] than to start from the one-particle wave equation [20]. We first introduce the "particle-field" Heisenberg operators, $\Psi_\alpha(x), \Psi^\dagger_\alpha(x)$, where α is the spin index and the $(1+2)$D spacetime coordinate $x \equiv (x^0, \boldsymbol{x})$. Note that x^0 is the time coordinate t and $\boldsymbol{x}$ is the spatial coordinate $\boldsymbol{r}$ in the main text. These operators satisfy the equal-time anticommutation relations:

$$\{\Psi_\alpha(x), \Psi^\dagger_{\alpha'}(x')\}|_{x^0=x'^0} = \delta^2(\boldsymbol{x}-\boldsymbol{x}')\delta_{\alpha\alpha'} \tag{A1}$$

and

$$\{\Psi_\alpha(x), \Psi_{\alpha'}(x')\}|_{x^0=x'^0} = \{\Psi^\dagger_\alpha(x), \Psi^\dagger_{\alpha'}(x')\}|_{x^0=x'^0} = 0. \tag{A2}$$

The quantized Hamiltonian is

$$\begin{aligned} H =& H_0 + H', \\ H_0 =& \int d^2\boldsymbol{x} \Psi^\dagger_\alpha(x)(-i\boldsymbol{\sigma}\cdot\nabla + m\sigma^z)_{\alpha\beta}\Psi_\beta(x), \\ H' =& \int d^2\boldsymbol{x} V(\boldsymbol{x})\Psi^\dagger_\alpha(x)\Psi_\alpha(x). \end{aligned} \tag{A3}$$

Recall that $V(\boldsymbol{x})$ is the disorder potential and the Einstein summation convention is applied to the spin indices. The Dirac system described by this Hamiltonian obeys the following current conservation law:

$$\begin{aligned} \partial_\mu j^\mu = 0, \\ j^0 = \Psi^\dagger_\alpha\Psi_\alpha, \quad \boldsymbol{j} = \Psi^\dagger_\alpha \boldsymbol{\sigma}_{\alpha\beta}\Psi_\beta. \end{aligned} \tag{A4}$$

Here $\partial_\mu \equiv (\partial_{x^0}, \nabla)$. Throughout this appendix it acts on the spacetime coordinate x, whenever several distinct spacetime coordinates (e.g., y, z, etc.) appear. By using Eqs. (A1) and (A2), it is easy to show that this conservation law entails the following identity:

$$\begin{aligned} &\partial_\mu\langle\Omega|\mathrm{T}\{j^\mu(x)\Psi_\alpha(y)\Psi^\dagger_\beta(z)\}|\Omega\rangle \\ =& -\delta^3(x-y)\langle\Omega|\mathrm{T}\{\Psi_\alpha(x)\Psi^\dagger_\beta(z)\}|\Omega\rangle \\ &+\delta^3(x-z)\langle\Omega|\mathrm{T}\{\Psi_\alpha(y)\Psi^\dagger_\beta(x)\}|\Omega\rangle. \end{aligned} \tag{A5}$$

Here Ω stands for the (many-body) ground state for a single disorder configuration, and "T" stands for the time-ordering operator.

To proceed we introduce the following representation, which is similar to the interaction representation but with the absence of the particle interaction. This allows us to bring the standard diagrammatic technique developed in the interaction representation for treating particle interactions to the present context to treat disorder potentials. Specifically, upon switching to the new presentation, a Heisenberg operator $F(t)$ is transformed to $\tilde{F}(t)$:

$$\tilde{F}(t) = S(t)F(t)S^{-1}(t), \quad S(t) := \mathrm{T}e^{-i\int_{-\infty}^{t}\tilde{H}'(t')dt'}, \tag{A6}$$

where

$$\tilde{H}'(t) = \int d^2\boldsymbol{x} V(\boldsymbol{x})\tilde{\Psi}^\dagger_\alpha(x)\tilde{\Psi}_\alpha(x). \tag{A7}$$

Similar to the interacting case [19], the ground state Ω can be expressed in terms of the ground state in the absence of the disorder potential, which is denoted as 0, via $S(t)$. As a result, for a generic product of Heisenberg operators, denoted as $\mathcal{O}$, we have:

$$\langle\Omega|\mathrm{T}\{\mathcal{O}\}|\Omega\rangle = \frac{\langle 0|\mathrm{T}\{\tilde{\mathcal{O}}S(\infty)\}|0\rangle}{\langle 0|S(\infty)|0\rangle}. \tag{A8}$$

Applying this formula to Eq. (A5) and dropping out the common denominator $\langle 0|S(\infty)|0\rangle$, we obtain:

$$\begin{aligned} &\partial_\mu\langle 0|\mathrm{T}\{\tilde{j}^\mu(x)\tilde{\Psi}_\alpha(y)\tilde{\Psi}^\dagger_\beta(z)S(\infty)\}|0\rangle \\ =& -\delta^3(x-y)\langle 0|\mathrm{T}\{\tilde{\Psi}_\alpha(x)\tilde{\Psi}^\dagger_\beta(z)S(\infty)\}|0\rangle \\ &+\delta^3(x-z)\langle 0|\mathrm{T}\{\tilde{\Psi}_\alpha(y)\tilde{\Psi}^\dagger_\beta(x)S(\infty)\}|0\rangle. \end{aligned} \tag{A9}$$

Let us substitute Eq. (A7) into Eq. (A9). Upon expanding the expression in $V(\boldsymbol{x})$, Feynman diagrams result. It should be emphasized that these diagrams have nothing to do with the disorder average and thereby have nothing to do with the Feynman diagrams resulting from the disorder average. Then, each term in Eq. (A9) can be organized as the product of the sum of all connected diagrams and a common factor arising from subdiagrams, which does not involve the external lines and are disconnected from the part that is connected and includes the external lines. This common factor can be found to be $\langle 0|S(\infty)|0\rangle$ by standard methods [18, 19]. So Eq. (A9) is reduced to:

$$\begin{aligned} &\partial_\mu\langle 0|\mathrm{T}\{\tilde{j}^\mu(x)\tilde{\Psi}_\alpha(y)\tilde{\Psi}^\dagger_\beta(z)S(\infty)\}|0\rangle_c \\ =& -\delta^3(x-y)\langle 0|\mathrm{T}\{\tilde{\Psi}_\alpha(x)\tilde{\Psi}^\dagger_\beta(z)S(\infty)\}|0\rangle_c \\ &+\delta^3(x-z)\langle 0|\mathrm{T}\{\tilde{\Psi}_\alpha(y)\tilde{\Psi}^\dagger_\beta(x)S(\infty)\}|0\rangle_c, \end{aligned} \tag{A10}$$

where the subscript "c" stands for that the diagrams are connected. The time-ordered Green's function in the ground state Ω is defined as:

$$G_{\alpha\beta}(x,y) = -i\langle\Omega|\mathrm{T}\{\tilde{\Psi}_\alpha(x)\tilde{\Psi}^\dagger_\beta(y)\}|\Omega\rangle, \tag{A11}$$

which is found to be

$$G_{\alpha\beta}(x,y) = i\langle 0|\mathrm{T}\{\tilde{\Psi}_\alpha(x)\tilde{\Psi}^\dagger_\beta(y)S(\infty)\}|0\rangle_c. \tag{A12}$$

Taking this into account we can rewrite Eq. (A10) as

$$\begin{aligned} &-i\partial_\mu\langle 0|\mathrm{T}\{\tilde{j}^\mu(x)\tilde{\Psi}_\alpha(y)\tilde{\Psi}^\dagger_\beta(z)S(\infty)\}|0\rangle_c \\ =& -\delta^3(x-y)G_{\alpha\beta}(x,z) + \delta^3(x-z)G_{\alpha\beta}(y,x). \end{aligned} \tag{A13}$$

Note that this result is for a single disorder configuration.

Now we wish to perform the disorder average of Eq. (A13). We first note that any V in a Feynman diagram defined above has to be uniquely paired with another V according to the rule: $\langle V(\boldsymbol{x})V(\boldsymbol{x}')\rangle = U_0\delta(\boldsymbol{x}-\boldsymbol{x}')$, so that the diagram can survive under the averaging. This effectively introduces the "statistical interaction" in term of Ref. [13] to each diagram and is represented by a dashed line (see Fig. 2 in the main text), which is often called the disorder scattering or impurity line in condensed matter physics. Upon this averaging the translational invariance is restored. So the average of the free Green's function, $\langle G_{\alpha\beta}(x,y)\rangle$, depends only on the difference of two space-time coordinates $x-y$, which is denoted as $\mathcal{G}_{\alpha\beta}(x-y)$. Therefore, upon the averaging a new kind of Feynman diagrams result, which are composed of $\mathcal{G}_{\alpha\beta}$ and the statistical interaction or the disorder scattering line. In the remainder of this appendix we consider this kind of Feynman diagrams.

For $\langle 0|\mathrm{T}\{\tilde{j}^\mu(x)\tilde{\Psi}_\alpha(y)\tilde{\Psi}^\dagger_\beta(z)S(\infty)\}|0\rangle_c$ its disorder average takes the following form:

$$\langle\langle 0|\mathrm{T}\{\tilde{j}^\mu(x)\tilde{\Psi}_\alpha(y)\tilde{\Psi}^\dagger_\beta(z)S(\infty)\}|0\rangle_c\rangle = \iint d^3y'd^3z'\mathcal{G}_{\alpha\alpha'}(y-y')(\Gamma^\mu)_{\alpha'\beta'}(y'|x|z')\mathcal{G}_{\beta'\beta}(z'-z), \tag{A14}$$

where $(\Gamma^\mu)_{\alpha\beta}(y|x|z)$ is the irreducible vertex function composed of irreducible diagrams. Here by "irreducible" it means that one cannot cut a free Green's function line to divide a diagram into two disconnected parts. We take the derivative with respect to x for both sides of Eq. (A14). With the help of the identity Eq. (A5), we find that

$$i\partial_\mu \iint d^3y'd^3z'\mathcal{G}_{\alpha\alpha'}(y-y')(\Gamma^\mu)_{\alpha'\beta'}(y'|x|z')\mathcal{G}_{\beta'\beta}(z'-z) = \delta^3(x-y)\mathcal{G}_{\alpha\beta}(x-z) - \delta^3(x-z)\mathcal{G}_{\alpha\beta}(y-x), \tag{A15}$$

which gives the Ward-Takahashi identity:

$$i\partial_\mu(\Gamma^\mu)_{\alpha'\beta'}(y'|x|z') = \mathcal{G}^{-1}_{\alpha'\beta'}(y'-x)\delta^3(x-z') - \delta^3(y'-x)\mathcal{G}^{-1}_{\alpha'\beta'}(x-z'). \tag{A16}$$

We show below that this identity results in a Vollhardt-Wölfle type Ward identity.

Note that the irreducible vertex function satisfies the following integral equation:

$$\begin{aligned}&(\Gamma^\mu)_{\alpha\beta}(y|x|z) - (\Gamma^\mu_0)_{\alpha\beta}(y|x|z)\\ &= -\iiiint d^3y_1d^3z_1d^3y_2d^3z_2\mathcal{G}_{\alpha_2\alpha_1}(y_2-y_1)(\Gamma^\mu)_{\alpha_1\beta_1}(y_1|x|z_1)\mathcal{G}_{\beta_1\beta_2}(z_1-z_2)U_{\beta_2\beta,\alpha\alpha_2}(y_2,z_2;y,z)\,,\end{aligned} \tag{A17}$$

where U is the Bethe-Salpeter kernel, and Γ^μ_0 is the bare vertex function, which is the one corresponding to the case where the statistical interaction is absent. Taking the derivative with respect to x for both sides and using the following fact:

$$\int d^3y\left((\mathcal{G}_0^{-1})(x-y) - \Sigma(x-y)\right)_{\alpha\beta}\mathcal{G}_{\beta\gamma}(y-z) = \delta^3(x-z)\delta_{\alpha\gamma}, \tag{A18}$$

we obtain:

$$\begin{aligned}&\Sigma_{\alpha\beta}(y-x)\delta^3(x-z) - \delta^3(y-x)\Sigma_{\alpha\beta}(x-z)\\ &= \iint d^3y_2d^3z_2\left(\delta^3(y_2-x)\mathcal{G}_{\alpha_2\beta_2}(x-z_2) - \mathcal{G}_{\alpha_2\beta_2}(y_2-x)\delta^3(x-z_2)\right)U_{\beta_2\beta,\alpha\alpha_2}(y_2,z_2;y,z).\end{aligned} \tag{A19}$$

Then we pass to the Fourier representation. The Fourier transformations of Green's function and the self-energy are

$$\mathcal{G}(x-y) = \int\frac{d^3k}{(2\pi)^3}e^{ik^\mu(x-y)_\mu}\mathcal{G}_{k^0}(\boldsymbol{k}), \quad \Sigma(x-y) = \int\frac{d^3k}{(2\pi)^3}e^{ik^\mu(x-y)_\mu}\Sigma_{k^0}(\boldsymbol{k}), \tag{A20}$$

respectively, where the spin indices have been omitted to make the formulae compact. To pass to the Fourier representation of the Bethe-Salpeter kernel U, it is important to note that the disorder potential has no time dependence and the translational invariance is restored, as a result of which U has to satisfy:

$$U(x',y';x,y) \equiv U(x'-x,y'-y,\boldsymbol{x}'-\boldsymbol{y}'), \tag{A21}$$

where we have omitted the spin indices since they are irrelevant for this constraint. Due to this constraint the Fourier transformation of U takes the following form:

$$U(x,'y';x,y) = \iiint\frac{d^3k_1}{(2\pi)^3}\frac{d^3k_2}{(2\pi)^3}\frac{d^2\boldsymbol{k}}{(2\pi)^2}e^{-i(k_1+\boldsymbol{k})^\mu x'_\mu+ik_1^\mu x_\mu}e^{i(k_2+\boldsymbol{k})^\mu y'_\mu-ik_2^\mu y_\mu}U(k_1+\boldsymbol{k},k_2+\boldsymbol{k};k_1,k_2), \tag{A22}$$

where we have used the shorthand notation: $k_{1,2}+\boldsymbol{k}\equiv(k^0_{1,2},\boldsymbol{k}_{1,2}+\boldsymbol{k})$. With the insertion of Eqs. (A20) and (A22), the left-hand side of Eq. (A19) is transformed to:

$$\iint \frac{d^3k_1}{(2\pi)^3}\frac{d^3k_2}{(2\pi)^3}e^{ik_1^\mu(y-x)_\mu}e^{ik_2^\mu(x-z)_\mu}\left(\Sigma_{k_1^0}(\boldsymbol{k}_1)-\Sigma_{k_2^0}(\boldsymbol{k}_2)\right)_{\alpha\beta} \tag{A23}$$

and the right-hand side to:

$$\iiint \frac{d^3k_1}{(2\pi)^3}\frac{d^3k_2}{(2\pi)^3}\frac{d^2\mathbf{k}}{(2\pi)^2}e^{ik_1^\mu(y-x)_\mu}e^{ik_2^\mu(x-z)_\mu}\left(\mathcal{G}_{k_2^0}(\boldsymbol{k}_2+\boldsymbol{k})-\mathcal{G}_{k_1^0}(\boldsymbol{k}_1+\boldsymbol{k})\right)_{\alpha_2\beta_2}U_{\beta_2\beta,\alpha\alpha_2}(k_1+\boldsymbol{k},k_2+\boldsymbol{k};k_1,k_2). \tag{A24}$$

Thus Eq. (A19) is transformed to:

$$\left(\Sigma_{k_1^0}(\boldsymbol{k}_1)-\Sigma_{k_2^0}(\boldsymbol{k}_2)\right)_{\alpha\beta}=\int\frac{d^2\boldsymbol{k}}{(2\pi)^2}\left(\mathcal{G}_{k_1^0}(\boldsymbol{k}_1+\boldsymbol{k})-\mathcal{G}_{k_2^0}(\boldsymbol{k}_2+\boldsymbol{k})\right)_{\alpha_2\beta_2}U_{\beta_2\beta,\alpha\alpha_2}(k_1+\boldsymbol{k},k_2+\boldsymbol{k};k_1,k_2). \tag{A25}$$

This may be considered as the most general Ward identity of Vollhardt-Wölfle type in disordered spin systems.

Let us consider a special case of Eq. (A25), where k_1^0 (k_2^0) is above (below) the Fermi energy. For the former (latter) we have $\mathcal{G}=\mathcal{G}^R$ ($\mathcal{G}=\mathcal{G}^A$) [18]. Substituting it into Eq. (A25), we obtain:

$$\left(\Sigma^R_{k_1^0}(\boldsymbol{k}_1)-\Sigma^A_{k_2^0}(\boldsymbol{k}_2)\right)_{\alpha\beta}=\int\frac{d^2\boldsymbol{k}'}{(2\pi)^2}\left(\mathcal{G}^R_{k_1^0}(\boldsymbol{k}_1+\boldsymbol{k}')-\mathcal{G}^A_{k_2^0}(\boldsymbol{k}_2+\boldsymbol{k}')\right)_{\alpha_2\beta_2}U_{\beta_2\beta,\alpha\alpha_2}(k_1+\boldsymbol{k}',k_2+\boldsymbol{k}';k_1,k_2). \tag{A26}$$

Denote $k^0_{1,2}=\varepsilon_\pm=\varepsilon\pm\frac{\omega}{2}$, $\boldsymbol{k}_{1,2}=\boldsymbol{k}_\pm=\boldsymbol{k}\pm\frac{\boldsymbol{q}}{2}$ and $\boldsymbol{p}=\boldsymbol{k}+\boldsymbol{k}'$, and the ensuing U as follows:

$$U_{\beta_2\beta,\alpha\alpha_2}(\varepsilon_+,\boldsymbol{p}_+,\varepsilon_-,\boldsymbol{p}_-;\varepsilon_+,\boldsymbol{k}_+,\varepsilon_-,\boldsymbol{k}_-)\equiv U^{\boldsymbol{pk}}_{\beta_2\beta,\alpha\alpha_2}(\boldsymbol{q},\omega), \tag{A27}$$

where we have omitted the parameter ε to make the expression compact. Then Eq. (A26) gives the Vollhardt-Wölfle type Ward identity, namely, Eq. (S9) or Eq. (7) in the main text. When all spin indices are suppressed the Ward identity derived by Vollhardt and Wölfle [11] is recovered.

APPENDIX B. PROOF OF EQ. (S72)

In this appendix we prove Eq. (S72). To start we note that $\phi^{\boldsymbol{pp}'}_{\alpha\beta,\beta'\alpha'}(\boldsymbol{q},\omega)$ can be diagrammatically represented by Fig. S4. By using Eq. (S14) we have:

$$\begin{aligned}(-2\pi i)\phi_0=&\Big(\sum_{\boldsymbol{p}}R^{\boldsymbol{p}}+\sum_{\boldsymbol{p},\boldsymbol{p}'}Z^{\boldsymbol{pp}'}+\sum_{\boldsymbol{p},\boldsymbol{p}'}R^{\boldsymbol{p}}\Gamma_0^{\boldsymbol{pp}'}R^{\boldsymbol{p}'}+\sum_{\boldsymbol{p},\boldsymbol{p}',\boldsymbol{k}_1}R^{\boldsymbol{p}}\Gamma_0^{\boldsymbol{pk}_1}Z^{\boldsymbol{k}_1\boldsymbol{p}'}+\sum_{\boldsymbol{p},\boldsymbol{p}',\boldsymbol{k}_1}Z^{\boldsymbol{pk}_1}\Gamma_0^{\boldsymbol{k}_1\boldsymbol{p}'}R^{\boldsymbol{p}'}\\&+\sum_{\boldsymbol{p},\boldsymbol{p}',\boldsymbol{k}_1,\boldsymbol{k}_2}R^{\boldsymbol{p}}\Gamma_0^{\boldsymbol{pk}_1}Z^{\boldsymbol{k}_1\boldsymbol{k}_2}\Gamma_0^{\boldsymbol{k}_2\boldsymbol{p}'}R^{\boldsymbol{p}'}\Big)_{\alpha\beta,\beta\alpha}.\end{aligned} \tag{B1}$$

Since $\Gamma_0^{\boldsymbol{pp}'}$ has no $\boldsymbol{p}$,$\boldsymbol{p}'$ dependence, Eq. (B1) can be simplified to:

$$(-2\pi i)\phi_0=\left(\tilde{R}+\tilde{Z}+\tilde{R}\Gamma_0\tilde{R}+\tilde{R}\Gamma_0\tilde{Z}+\tilde{Z}\Gamma_0\tilde{R}+\tilde{R}\Gamma_0\tilde{Z}\Gamma_0\tilde{R}\right)_{\alpha\beta,\beta\alpha}. \tag{B2}$$

where

$$\tilde{R}=\sum_{\boldsymbol{p}}R^{\boldsymbol{p}},\qquad \tilde{Z}=\sum_{\boldsymbol{p},\boldsymbol{p}'}Z^{\boldsymbol{pp}'}. \tag{B3}$$

Multiplying both sides of Eq. (B2) by U_0 and using the first line of the following identity:

$$\begin{aligned}(\Gamma_0)_{\alpha\beta,\beta'\alpha'}=&U_0\delta_{\alpha\beta}\delta_{\beta'\alpha'}+U_0\left(\tilde{R}\Gamma_0\right)_{\alpha\beta,\beta'\alpha'}\\=&U_0\delta_{\alpha\beta}\delta_{\beta'\alpha'}+U_0\left(\Gamma_0\tilde{R}\right)_{\alpha\beta,\beta'\alpha'},\end{aligned} \tag{B4}$$

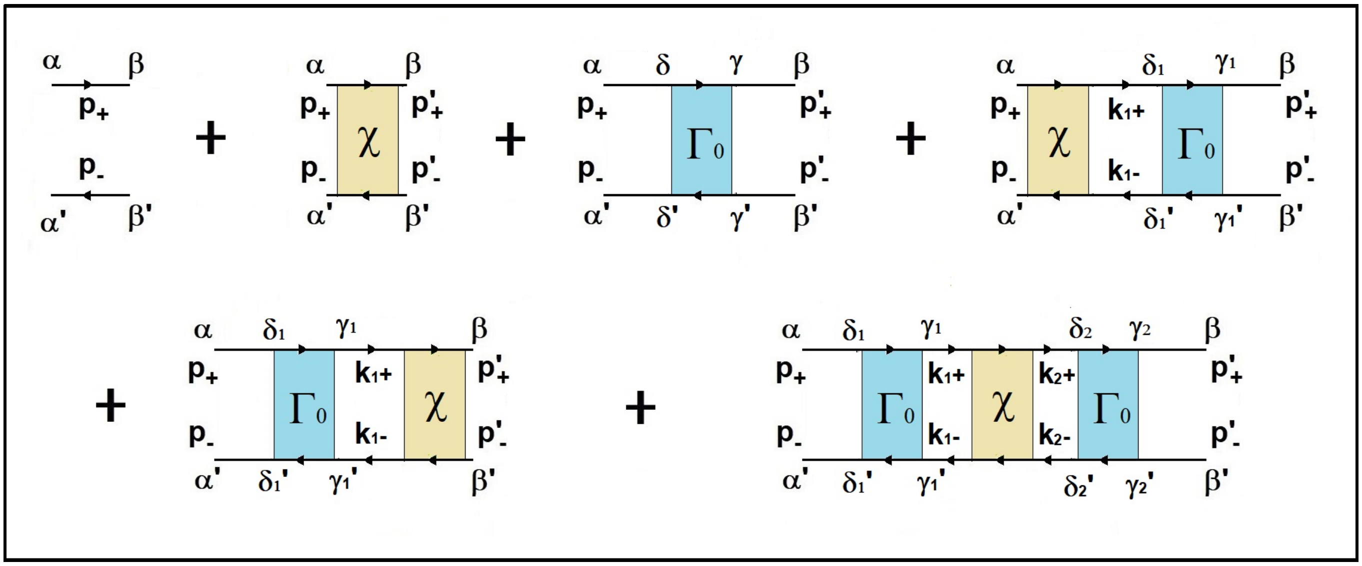

Fig. S4. Diagrammatical representation of $\phi^{\boldsymbol{pp'}}_{\alpha\beta,\beta'\alpha'}(\boldsymbol{q},\omega)$.

we obtain:

$$\begin{aligned}(-2\pi i)U_0\phi_0 &= \Big(U_0\tilde{R} + U_0\tilde{Z} + U_0\tilde{R}\Gamma_0\tilde{R} + U_0\tilde{R}\Gamma_0\tilde{Z} + U_0\tilde{Z}\Gamma_0\tilde{R} + (\Gamma_0 - U_0)\tilde{Z}\Gamma_0\tilde{R}\Big)_{\alpha\beta,\beta\alpha} \\ &= \Big(U_0\tilde{R} + U_0\tilde{Z} + U_0\tilde{R}\Gamma_0\tilde{R} + U_0\tilde{R}\Gamma_0\tilde{Z} + \Gamma_0\tilde{Z}\Gamma_0\tilde{R}\Big)_{\alpha\beta,\beta\alpha}. \end{aligned} \tag{B5}$$

Multiplying both sides of Eq. (B5) by U_0 and using Eq. (B4), we obtain:

$$\begin{aligned}(-2\pi i)U_0^2\phi_0 &= \Big(U_0^2\tilde{R} + U_0^2\tilde{Z} + U_0^2\tilde{R}\Gamma_0\tilde{R} + U_0(\Gamma_0 - U_0)\tilde{Z} + \Gamma_0\tilde{Z}(\Gamma_0 - U_0)\Big)_{\alpha\beta,\beta\alpha} \\ &= \Big(U_0^2\tilde{R} + U_0^2\tilde{R}\Gamma_0\tilde{R} + \Gamma_0\tilde{Z}\Gamma_0\Big)_{\alpha\beta,\beta\alpha}. \end{aligned} \tag{B6}$$

Applying the first line of Eq. (B4) to the second term of Eq. (B6), we obtain:

$$(-2\pi i)U_0^2\phi_0 = \Big(U_0\Gamma_0\tilde{R} + \Gamma_0\tilde{Z}\Gamma_0\Big)_{\alpha\beta,\beta\alpha}. \tag{B7}$$

Applying the second line of Eq. (B4) to the first term of Eq. (B7) we further obtain:

$$(-2\pi i)U_0^2\phi_0 = \Big(\Gamma_0 - U_0 + \Gamma_0\tilde{Z}\Gamma_0\Big)_{\alpha\beta,\beta\alpha}, \tag{B8}$$

which is Eq. (S72).

*E-mail: ct@itp.ac.cn

[1] K. B. Efetov, *Supersymmetry in Disorder and Chaos* (Cambridge University Press, Cambridge, 1997).
[2] P. M. Ostrovsky, I. V. Gornyi, and A. D. Mirlin, Phys. Rev. Lett. **98**, 256801 (2007).
[3] G. Tkachov, *Topological Insulators: The Physics of Spin Helicity in Quantum Transport* (Pan Stanford Publishing, Singapore, 2016).
[4] I. V. Gornyi, V. Yu. Kachorovskii, and P. M. Ostrovsky, Phys. Rev. B **90**, 085401 (2014).
[5] K. Nomura, M. Koshino, and S. Ryu, Phys. Rev. Lett. **99**, 146806 (2007).
[6] J. H. Bardarson, J. Tworzydlo, P. W. Brouwer, and C. W. J. Beenakker, Phys. Rev. Lett. **99**, 106801 (2007).
[7] S. Hikami, A. I. Larkin, and Y. Nagaoka, Prog. Theor. Phys. **63**, 707 (1980).
[8] C. Tian, Phys. Rev. B. **86**,121304R (2012)
[9] I. A. Ado, I. A. Dmitriev, P. M. Ostrovsky, and M. Titov,

Europhys. Lett. **111**, 37004 (2015).
[10] F. J. Dyson, J. Math. Phys. **3**, 140 (1962).
[11] D.Vollhardt and P. Wölfle, Phys. Rev. B. **22**, 4666 (1980).
[12] D. Vollhardt and P. Wölfle, in *Electronic Phase Transitions*, edited by W. Hanke and Yu. V. Kopaev (North-Holland, Amsterdam, 1992),pp. 1-78
[13] H. T. Nieh, P. Sheng, and X. B. Wang, Phys. Lett. A **246**, 542 (1998).
[14] H. T. Nieh, L. Chen, and P. Sheng, Phys. Rev. E **57**, 1145 (1998).
[15] L. Erdös, M. Salmhofer and H. T. Yau, in *Mathematical Physics of Quantum Mechanics: Selected and Refereed Lectures from QMath9* edited by J. Asch and A. Joye, Lecture Notes in Physics Vol. **690**, (Springer, Heidelberg, 2006), pp.233-258
[16] L. Erdös, M. Salmhofer and H. T. Yau, Commun. Math. Phys. **271**, 1, (2007).
[17] E. Abrahams, P. W. Anderson, D. C. Licciardello and T. V. Ramakrishnan, Phys. Rev. Lett. **42**, 673 (1979).
[18] A. A. Abrikosov, L. P. Gorkov and I. Ye. Dzyaloshinskii, *Quantum Field Theoretical Methods in Statistical Physics*, 2nd Ed. (Pergamon, Oxford, 1965).
[19] M. E. Peskin and D. V. Schroeder, *An Introduction to Quantum Field Theory* (Perseus, Cambridge, 1995).
[20] P. Sheng, *Introduction to Wave Scattering, Localization, and Mesoscopic Phenomena*, 2nd Ed. (Springer, Berlin, Germany, 2006).